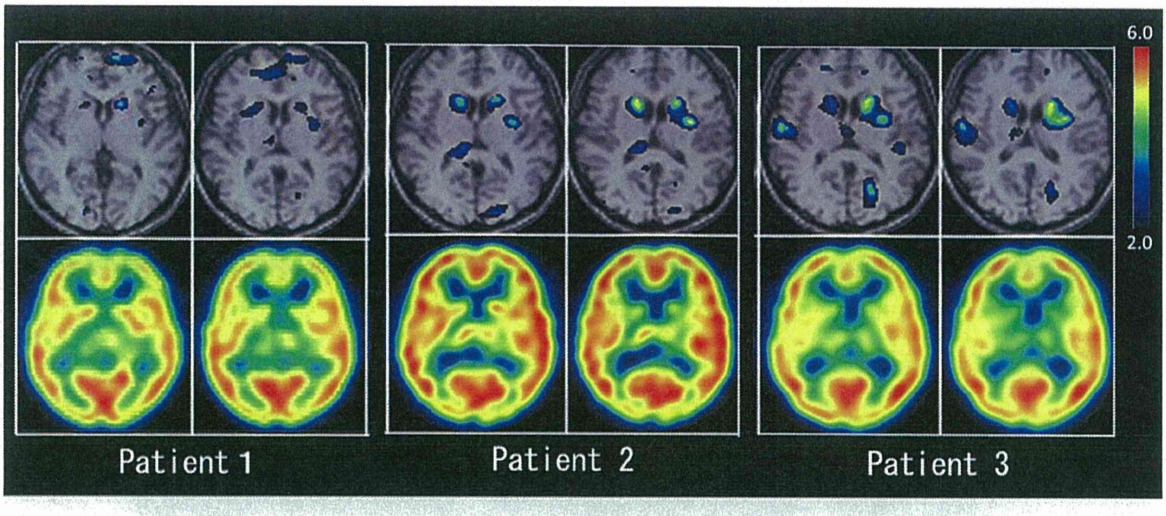

Fig. 2. ECD-SPECT and eZIS results.Usual color images of ECD-SPECT in three patients were shown on the lower figures in each patient. Analyzed images using eZIS were shown on the upper figures. The converted images indicate regions of decreased cerebral blood flow by colors from blue (2.0 standard deviation) to red (6.0 standard deviation). Reduction in cerebral blood flow was shown most common and prominent in the bilateral caudate nuclei in all three patients.

(data not shown), we could not discriminate visible areas of abnormal cerebral perfusion or glucose metabolism. However, the statistical analysis of the ECD-SPECT data using eZIS demonstrated significant declines in cerebral blood flow in the basal ganglia, especially in the caudate nuclei (Fig. 2, upper figure). Although several other brain regions were shown to have decreased blood flow, these were not shared in the three patients.

Array CGH analysis revealed that Patient 1 had an approximately 2.6-Mb hemizygous deletion including *NKX2-1* in 14q12–13 (Fig. 3, top). Direct sequencing analysis revealed a novel hemizygous mutation in the coding exons in Patients 2 and 3 (Fig. 3, bottom), but no mutation in Patient 1. A hemizygous G-to-T substitution at nucleotide position 613 (c.613G>T) in Patients 2 and 3 created an amino acid substitution at amino acid position 205 (p.Val205Phe) within exon 3, which is localized within the *NKX2-1* homeodomain. The mothers and grandmother of Patients 2 and 3 had the same missense mutation.

4. Discussion

In this study, we diagnosed three children with brain–lung–thyroid syndrome based on clinical findings of delayed walking, unsteady gait, choreoathetosis, and hypothyroidism. The diagnosis was confirmed by genetic analysis detecting a novel hemizygous deletion and missense mutations in *NKX2-1*. In addition, we performed nuclear image examinations and analyzed the results using statistical image analysis with eZIS. We found a significant reduction in the blood flow in the caudate nuclei in all three patients.

Recurrent respiratory infection was observed only in the patient with the deletion in *NKX2-1*, but not in the two patients with missense mutations. These phenotype-genotype correlations support previous reports [8,10–13] that large deletions and truncation mutations are related to the severe phenotype with the symptom triad, while missense mutations have a milder phenotype [13]. The existence of respiratory symptoms is very important for management because no deaths have been reported in patients without lung disease [12]. In one case with a missense mutation, hypothyroidism was not detected until the age of 5 years, while it was detected in his cousin with the same mutation at neonatal screening. This interfamilial heterogeneity, as described previously [25], indicates that simple haploinsufficiency cannot fully explain the spectrum of clinical presentations. Other modifying genes might contribute to the phenotype heterogeneity [9,12].

Central nervous impairment is the most common and essential symptom in brain–lung–thyroid syndrome [12,13]. Typically, mental retardation and brain MRI abnormalities are not associated with this disease. The characteristic presentation involves delayed walking, a staggering gait, and choreoathetosis. Since no obvious nervous system abnormalities were detected on neurological examinations, we speculate that the choreoathetosis in the lower limbs caused the delay in walking and unsteady gait.

To identify the brain region responsible for the neurological impairment, we examined brain ECD-SPECT and FDG-PET, but no obvious pathological abnormalities were detected on visual inspection of the raw images. Further statistical analysis of the ECD-SPECT data was performed using eZIS, while the FDG-PET was not analyzed because we did not have an appropriate analysis method. The eZIS method can detect a significant difference of regional cerebral blood flow by comparison with age-matched normal controls, and shows the result as color images. Previous reports described significant superiority of this program over visual inspection of raw SPECT images in several diseases [26–28]. We analyzed our patients and found a common, significant reduction in cerebral blood flow in the caudate nuclei. Although most reports describe expression of the *NKX2-1* gene in the pallidum [8,21,22], a recent study showed *NKX2-1* expression in the postnatal mouse striatum, including the caudate nuclei, in addition to the pallidum [29]. In humans, nuclear image studies indicated a reduction in blood flow [23] and glucose metabolism [15] in the basal ganglia. Hypoperfusion in the caudate nuclei was described in a patient with Huntington's disease [30,31], which usually involves chorea. From these reports and our ECD-SPECT findings using eZIS, we believe that the region responsible for the neurological symptoms in brain–lung–thyroid syndrome, pathologically, is the caudate nuclei. We speculate the possible mechanism that the mutation may impair developmental differentiation and organization of the striatum. Huntington's disease, which also involves the caudate nuclei, partially mimics brain–lung–thyroid syndrome clinically, although the latter is easily differentiated by the history of delayed walking.

In our cases, oral L-dopa [32], a dopamine agonist, and clonazepam failed to improve their neurological impairment. Only a few effective treatment for involuntary movement has been reported [13]. Although some reports described the choreatic movements tend to decrease over time [7,23], the movement disability causes severe trouble with daily life, especially writing difficulty resulting in a leaning impairment in

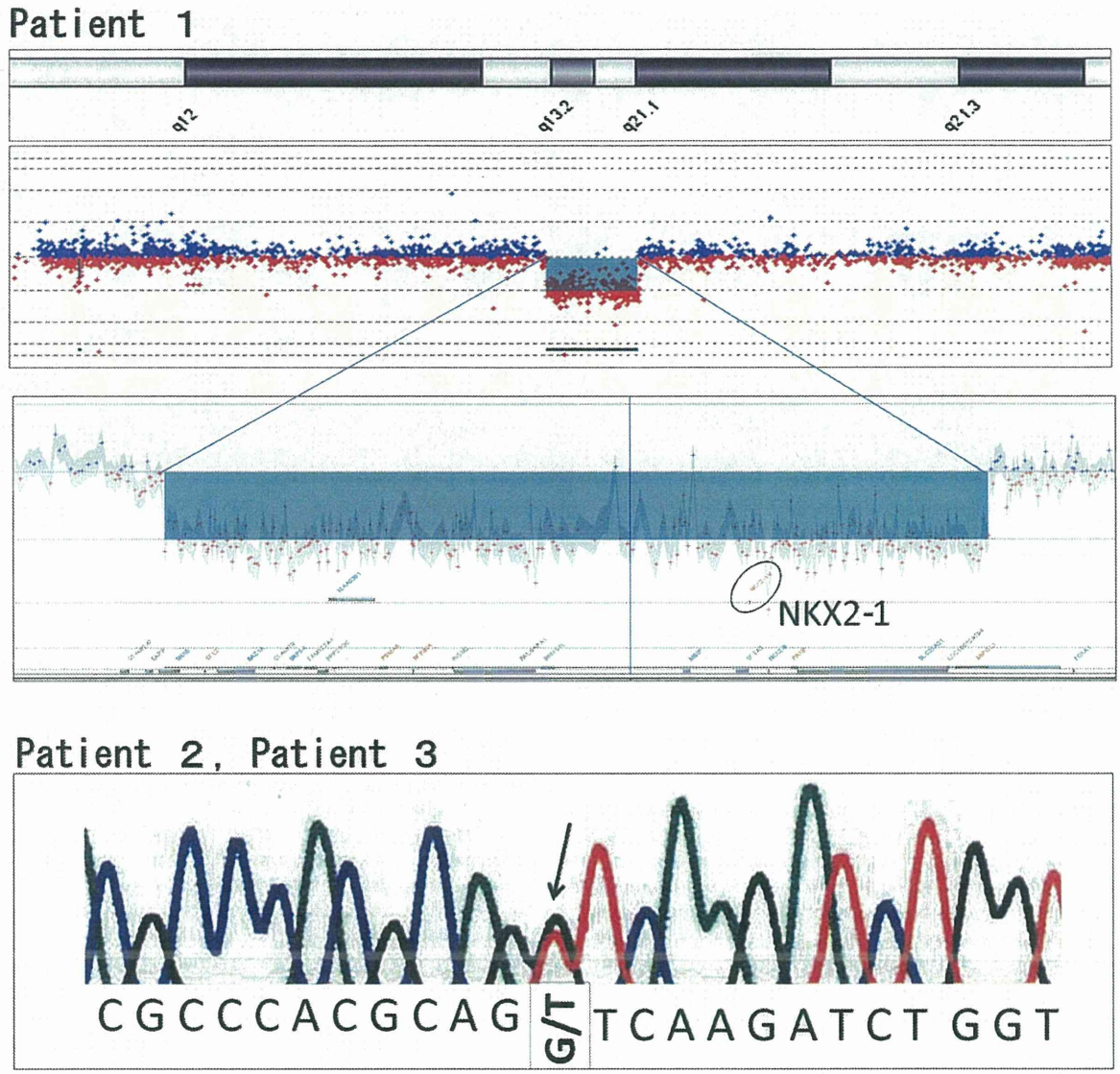

Fig. 3. Deletion and missense mutation in *NKX2-1*. Chromosome 14 profile and detail of 14q12–13 region generated by Cytogenomics (version 1.5, Agilent Technologies) showed a hemizygous 2.6-Mb deletion including *NKX2-1* in Patient 1. Sequencing analysis showed hemizygous missense mutations (c.613G>T) in *NKX2-1* in Patients 2 and 3.

childhood. We postulate that deep brain stimulation might treat involuntary movement, such as in Huntington's disease [33]. The pathophysiology of this disease should be clarified to develop an effective treatment.

Acknowledgments

We are grateful to Ms. Yoko Chiba and Ms. Kumi Itou for their technical assistance.

References

[1] Hamdan H, Liu H, Li C, Jones C, Lee M, deLemos R, et al. Structure of the human Nkx2.1 gene. Biochim Biophys Acta 1998;1396:336–48.
[2] Ikeda K, Clark JC, Shaw-White JR, Stahlman MT, Boutell CJ, Whitsett JA. Gene structure and expression of human thyroid transcription factor-1 in respiratory epithelial cells. J Biol Chem 1995;270:8108–14.
[3] Lazzaro D, Price M, de Felice M, Di Lauro R. The transcription factor TTF-1 is expressed at the onset of thyroid and lung morphogenesis and in restricted regions of the foetal brain. Development 1991;113:1093–104.
[4] Kimura S, Hara Y, Pineau T, Fernandez-Salguero P, Fox CH, Ward JM, et al. The T/ebp null mouse: thyroid-specific enhancer-binding protein is essential for the organogenesis of the thyroid, lung, ventral forebrain, and pituitary. Genes Dev 1996;10:60–9.
[5] Puelles L, Kuwana E, Puelles E, Bulfone A, Shimamura K, Keleher J, et al. Pallial and subpallial derivatives in the embryonic chick and mouse telencephalon, traced by the expression of the genes Dlx-2, Emx-1, Nkx-2.1, Pax-6, and Tbr-1. J Comp Neurol 2000;424:409–38.
[6] Acebron A, Aza-Blanc P, Rossi DL, Lamas L, Santisteban P. Congenital human thyroglobulin defect due to low expression of the thyroid-specific transcription factor TTF-1. J Clin Invest 1995;96:781–5.
[7] Breedveld GJ, van Dongen JW, Danesino C, Guala A, Percy AK, Dure LS, et al. Mutations in TITF-1 are associated with benign hereditary chorea. Hum Mol Genet 2002;11:971–9.
[8] Krude H, Schutz B, Biebermann H, von Moers A, Schnabel D, Neitzel H, et al. Choreoathetosis, hypothyroidism, and pulmonary alterations due to human NKX2-1 haploinsufficiency. J Clin Invest 2002;109:475–80.
[9] Breedveld GJ, Percy AK, MacDonald ME, de Vries BB, Yapijakis C, Dure LS, et al. Clinical and genetic heterogeneity in benign hereditary chorea. Neurology 2002;59:579–84.
[10] Willemsen MA, Breedveld GJ, Wouda S, Otten BJ, Yntema JL, Lammens M, et al. Brain–thyroid–lung syndrome: a patient with a severe multi-system disorder due to a de novo mutation in the thyroid transcription factor 1 gene. Eur J Pediatr 2005;164:28–30.
[11] Kleiner-Fisman G, Lang AE. Benign hereditary chorea revisited: a journey to understanding. Mov Disord 2007;22:2297–305 [quiz 452].
[12] Carre A, Szinnai G, Castanet M, Sura-Trueba S, Tron E, Broutin-L'Hermite I, et al. Five new TTF1/NKX2.1 mutations in brain–lung–thyroid syndrome: rescue by PAX8 synergism in one case. Hum Mol Genet 2009;18:2266–76.

[13] Inzelberg R, Weinberger M, Gak E. Benign hereditary chorea: an update. Parkinsonism Relat Disord 2011;17:301–7.
[14] Carmo Costa M, Costa C, Silva AP, Evangelista P, Santos L, Ferro A, et al. Nonsense mutation in TITF1 in a Portuguese family with benign hereditary chorea. Neurogenetics 2005;6:209–15.
[15] Salvatore E, Di Maio L, Filla A, Ferrara AM, Rinaldi C, Sacca F, et al. Benign hereditary chorea: clinical and neuroimaging features in an Italian family. Mov Disord 2010;25:1491–6.
[16] Butt SJB, Sousa VH, Fuccillo MV, Hjerling-Leffler J, Miyoshi G, Kimura S, et al. The requirement of Nkx2-1 in the temporal specification of cortical interneuron subtypes. Neuron 2008;59:722–32.
[17] Trueba SS. PAX8, TITF1, and FOXE1 gene expression patterns during human development: new insights into human thyroid development and thyroid dysgenesis-associated malformations. J Clin Endocrinol Metabol 2004;90:455–62.
[18] Maeda Y, Davé V, Whitsett J. Transcriptional control of lung morphogenesis. Physiol Rev 2007;87:219–44.
[19] Guillot L, Carré A, Szinnai G, Castanet M, Tron E, Jaubert F, et al. NKX2-1mutations leading to surfactant protein promoter dysregulation cause interstitial lung disease in "Brain–Lung–Thyroid Syndrome". Hum Mutat 2010;31:E1146–62.
[20] Glik A, Vuillaume I, Devos D, Inzelberg R. Psychosis, short stature in benign hereditary chorea: a novel thyroid transcription factor-1 mutation. Mov Disord 2008;23:1744–7.
[21] Sussel L, Marin O, Kimura S, Rubenstein JL. Loss of Nkx2.1 homeobox gene function results in a ventral to dorsal molecular respecification within the basal telencephalon: evidence for a transformation of the pallidum into the striatum. Development 1999;126:3359–70.
[22] Flandin P, Kimura S, Rubenstein JLR. The progenitor zone of the ventral medial ganglionic eminence requires Nkx2-1 to generate most of the globus pallidus but few neocortical interneurons. J Neurosci 2010;30:2812–23.
[23] Mahajnah M, Inbar D, Steinmetz A, Heutink P, Breedveld GJ, Straussberg R. Benign hereditary chorea: clinical, neuroimaging, and genetic findings. J Child Neurol 2007;22:1231–4.
[24] Kanetaka H, Matsuda H, Asada T, Ohnishi T, Yamashita F, Imabayashi E, et al. Effects of partial volume correction on discrimination between very early Alzheimer's dementia and controls using brain perfusion SPECT. Eur J Nucl Med Mol Imaging 2004;31:975–80.
[25] Montanelli L, Tonacchera M. Genetics and phenomics of hypothyroidism and thyroid dys- and agenesis due to PAX8 and TTF1 mutations. Mol Cell Endocrinol 2010;322:64–71.
[26] Matsuda H, Mizumura S, Nagao T, Ota T, Iizuka T, Nemoto K, et al. Automated discrimination between very early Alzheimer disease and controls using an easy Z-score imaging system for multicenter brain perfusion single-photon emission tomography. AJNR Am J Neuroradiol 2007;28:731–6.
[27] Imamura K, Wada-Isoe K, Kowa H, Tanabe Y, Nakashima K. The effect of donepezil on increased regional cerebral blood flow in the posterior cingulate cortex of a patient with Parkinson's disease dementia. Neurocase 2008;14:271–5.
[28] Sasaki M, Nakagawa E, Sugai K, Shimizu Y, Hattori A, Nonoda Y, et al. Brain perfusion SPECT and EEG findings in children with autism spectrum disorders and medically intractable epilepsy. Brain Dev 2010;32:776–82.
[29] Magno L, Catanzariti V, Nitsch R, Krude H, Naumann T. Ongoing expression of Nkx2.1 in the postnatal mouse forebrain: potential for understanding NKX2.1 haploinsufficiency in humans? Brain Res 2009;1304:164–86.
[30] Hasselbalch SG, Oberg G, Sorensen SA, Andersen AR, Waldemar G, Schmidt JF, et al. Reduced regional cerebral blood flow in Huntington's disease studied by SPECT. J Neurol Neurosurg Psychiatry 1992;55:1018–23.
[31] Reynolds Jr NC, Hellman RS, Tikofsky RS, Prost RW, Mark LP, Elejalde BR, et al. Single photon emission computerized tomography (SPECT) in detecting neurodegeneration in Huntington's disease. Nucl Med Commun 2002;23:13–8.
[32] Asmus F, Horber V, Pohlenz J, Schwabe D, Zimprich A, Munz M, et al. A novel TITF-1 mutation causes benign hereditary chorea with response to levodopa. Neurology 2005;64:1952–4.
[33] Kang GA, Heath S, Rothlind J, Starr PA. Long-term follow-up of pallidal deep brain stimulation in two cases of Huntington's disease. J Neurol Neurosurg Psychiatry 2010;82:272–7.

Human Molecular Genetics, 2012, Vol. 21, No. 7 *1496–1503*
doi:10.1093/hmg/ddr585
Advance Access published on December 13, 2011

Mutations in genes encoding the glycine cleavage system predispose to neural tube defects in mice and humans

Ayumi Narisawa[1,2], Shoko Komatsuzaki[1], Atsuo Kikuchi[3], Tetsuya Niihori[1], Yoko Aoki[1], Kazuko Fujiwara[4], Mitsuyo Tanemura[5], Akira Hata[6], Yoichi Suzuki[6], Caroline L. Relton[7], James Grinham[8], Kit-Yi Leung[8], Darren Partridge[8], Alexis Robinson[8], Victoria Stone[8], Peter Gustavsson[9], Philip Stanier[8], Andrew J. Copp[8], Nicholas D.E. Greene[8,*], Teiji Tominaga[2], Yoichi Matsubara[1] and Shigeo Kure[1,3,*]

[1]Department of Medical Genetics, [2]Department of Neurosurgery and [3]Department of Pediatrics, Tohoku University School of Medicine, Sendai, Japan, [4]Institute for Enzyme Research, University of Tokushima, Tokushima, Japan, [5]Tanemura Women's Clinic, Nagoya, Japan, [6]Department of Public Health, Chiba University School of Medicine, Chiba, Japan, [7]Human Nutrition Research Centre, Institute for Ageing and Health, Newcastle University, Newcastle upon Tyne, UK, [8]Institute of Child Health, University College London, London, UK and [9]Department of Molecular Medicine and Surgery, Karolinska Institute, Stockholm, Sweden

Received October 26, 2011; Revised November 25, 2011; Accepted December 6, 2011

Neural tube defects (NTDs), including spina bifida and anencephaly, are common birth defects of the central nervous system. The complex multigenic causation of human NTDs, together with the large number of possible candidate genes, has hampered efforts to delineate their molecular basis. Function of folate one-carbon metabolism (FOCM) has been implicated as a key determinant of susceptibility to NTDs. The glycine cleavage system (GCS) is a multi-enzyme component of mitochondrial folate metabolism, and GCS-encoding genes therefore represent candidates for involvement in NTDs. To investigate this possibility, we sequenced the coding regions of the GCS genes: *AMT*, *GCSH* and *GLDC* in NTD patients and controls. Two unique non-synonymous changes were identified in the *AMT* gene that were absent from controls. We also identified a splice acceptor site mutation and five different non-synonymous variants in *GLDC*, which were found to significantly impair enzymatic activity and represent putative causative mutations. In order to functionally test the requirement for GCS activity in neural tube closure, we generated mice that lack GCS activity, through mutation of *AMT*. Homozygous $Amt^{-/-}$ mice developed NTDs at high frequency. Although these NTDs were not preventable by supplemental folic acid, there was a partial rescue by methionine. Overall, our findings suggest that loss-of-function mutations in GCS genes predispose to NTDs in mice and humans. These data highlight the importance of adequate function of mitochondrial folate metabolism in neural tube closure.

INTRODUCTION

Neural tube defects (NTDs), such as spina bifida and anencephaly, are severe birth defects that result from failure of closure of the neural folds during embryonic development (1). Although NTDs are among the commonest birth defects in humans, the causes are still not well understood. This is most likely due to their complex, multifactorial causation

*To whom correspondence should be addressed at: Neural Development Unit, UCL Institute of Child Health, Guilford Street, London, WC1N 1EH, UK. Email: n.greene@ucl.ac.uk (N.D.E.G.); Department of Pediatrics, Tohoku University School of Medicine, 1-1 Seiryomachi, Aobaku, Sendai 980-8574, Japan. Email: kure@med.tohoku.ac.jp (S.Ku.)

which is thought to involve contributions from both genetic and environmental factors (2–4). The potential complexity of NTD genetics is illustrated by the fact that more than 200 different genes give rise to NTDs when mutated in mice (5,6). Moreover, inheritance patterns in humans suggest a multigenic model in which an affected individual may carry two or more risk alleles, which by themselves may be insufficient to cause NTDs (2).

Folate one-carbon metabolism (FOCM) is strongly implicated as a determinant of susceptibility to NTDs since suboptimal maternal folate status and/or elevated homocysteine are established risk factors, whereas periconceptional maternal folic acid supplementation can reduce the occurrence and recurrence of NTDs (7,8). Nevertheless, the precise mechanism by which folate status influences NTD risk remains elusive (7,9). FOCM comprises a network of enzymatic reactions required for synthesis of purines and thymidylate for DNA synthesis, and methionine, which is required for methylation of biomolecules (Fig. 1A) (9). In addition to the cytosol, FOCM also operates in mitochondria, supplying extra one-carbon units to the cytosolic FOCM as formate (Fig. 1A) (10).

Genes that are functionally related to folate metabolism have been subjected to intensive genetic analysis in relation to NTD causation, principally through association studies (reviewed in 3,4,11). In the most extensively studied gene, *MTHFR*, the c.677C>T SNP is associated with NTDs in some, but not all, populations. However, other FOCM-related genes have largely shown non-significant or only mild associations. Given the apparently complex inheritance of the majority of human NTDs, many association studies have been hampered by limitations on sample size. Moreover, although positive associations have been noted for other genes including *DHFR*, *MTHFD1*, *MTRR* and *TYMS* (12,13), these have not been replicated in all populations, and additional studies are required. The hypothesis that genetically determined abnormalities of folate metabolism may contribute to NTD susceptibility is supported by the observation of defects of thymidylate biosynthesis in a proportion of primary cell lines derived from NTDs (14). However, these defects do not correspond with known polymorphisms in FOCM-related genes. Overall, it appears likely that genetic influences on folate metabolism remain to be identified in many NTDs.

A potential link between mitochondrial FOCM and NTDs was suggested by the finding of an association of increased NTD risk with an intronic polymorphism in *MTHFD1L* (15). Another component of mitochondrial FOCM, the glycine cleavage system (GCS), acts to break down glycine to donate one-carbon units to tetrahydrofolate (THF), generating 5,10-methylenetetrahydrofolate (methylene-THF; Fig. 1B) (16,17). The GCS consists of four enzyme components, each of which is required for the glycine cleavage reaction (18,19). The components—glycine dehydrogenase (decarboxylating) (GLDC; P-protein), aminomethlyltransferase (AMT; T-protein), glycine cleavage system protein H (GCSH; H-protein) and dihydrolipoamide dehydrogenase (DLD; L-protein)—are encoded by distinct genes: *GLDC*, *AMT*, *GCSH* and *DLD*, respectively. The functions of *GLDC*, *AMT* and *GCSH* are specific to the GCS, whereas *DLD* encodes a housekeeping enzyme. GCS components have been found to be abundantly expressed in the neuroepithelium during embryogenesis in the rat (20).

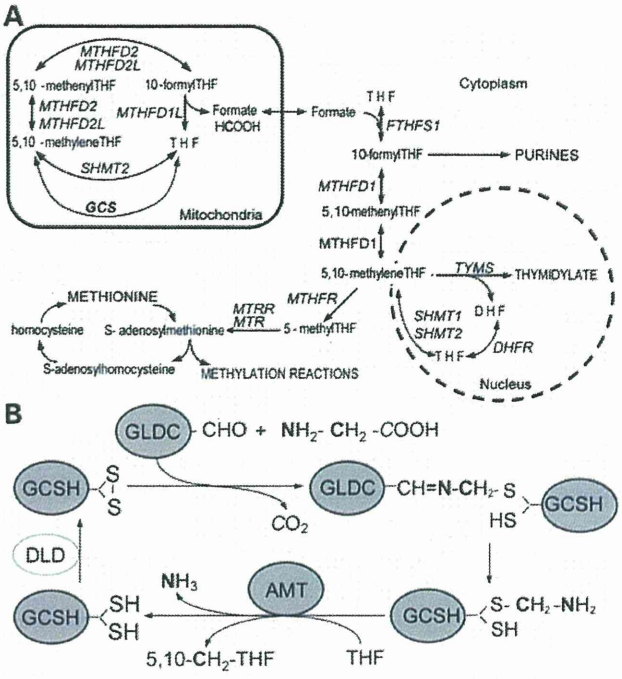

Figure 1. Schematic diagrams summarizing the key reactions of folate-mediated one-carbon metabolism and the GCS. (**A**) Folates donate and accept one-carbon units in the synthesis of purines, thymidylate and methionine. Mitochondrial FOCM supplies one-carbon units to the cytoplasm via formate. The GCS is a key component of mitochondrial FOCM that breaks down glycine and generates 5,10-methylene-THF from THF. Genes encoding enzymes for each reaction are indicated in italics. DHF, dihydrofolate; THF, tetrahydrofolate. (**B**) Summary of the GCS. The glycine cleavage reaction is catalysed by the sequential action of four individual enzymes: GLDC, GCSH, AMT and DLD. The first three of these (shaded grey) are specific to the GCS. Glycine is broken down into CO_2 and NH_3, and donates a one-carbon unit (indicated in bold) to THF, generating 5,10-methylene-THF. The other carbon in glycine (indicated in italics) enters CO_2.

We hypothesized that modulation of GCS activity has the potential to influence efficacy of cellular FOCM during the period of neural tube closure and, hence, susceptibility to NTDs. Therefore, in the current study, we screened genes encoding GCS components for possible mutations in NTD patients and controls. We tested variant proteins for loss of function by enzymatic assay and mice lacking GCS function were generated, to test the effect on embryonic development.

RESULTS

The hypothesis that genes of the GCS represent candidates for involvement in NTDs prompted us to screen for potential mutations in patient samples. Coding exons of *AMT* (9 exons), *GCSH* (5 exons) and *GLDC* (25 exons) were sequenced in a total of 258 NTD patients comprising cohorts from Japan, the UK and Sweden. Each of the major categories of NTDs was represented among study samples, including anencephaly ($n = 38$), spina bifida ($n = 198$) and craniorachischisis ($n = 22$).

Table 1. Nucleotide changes in NTD patients and controls identified by exon sequencing of AMT, GLDC and GCSH

Location	Nucleotide change	Effect	Number of mutation carriers in UK cohorts		Number of mutation carriers in the Japanese cohort		Number of mutation carriers in the Swedish cohort		Variant GLDC enzyme activity[a]
			NTD group (type[b]) ($n = 166$)[c]	Control group ($n = 189$)[c]	NTD group (type[b]) ($n = 14$)[c]	Control group ($n = 36$)[c]	NTD group (type[b]) ($n = 76$)[c]	Control group ($n = 145$)[c]	
AMT									
Exon 2	c.103A>C	p.R35R	0	1	0	0	0	—	
	c.214A>G	p.T72A	0	0	0	1	0	—	
Exon 6	c.623C>A	p.A208D	0	2	0	0	0	—	
	c.631G>A	p.E211K[d]	2 (SBA)	0	0	0	1	—	
	c.589G>C	p.D197H	0	0	1 (An)	0	0	—	
Exon 7	c.825T>A	p.N275K	0	1	0	0	0	—	
	c.850G>C	p.V284L	1 (SBA)	0	0	0	0	—	
GLDC									
Exon 1	c.52G>T	p.G18C	2 (SBO/SBA)	2	0	0	2 (SBA)	2	84%
Exon 5	c.668C>G	p.P223R	0	0	0	1	0	—	92%
Exon 12	c.1508A>C	p.E503A	1 (SBA)	0	0	0	0	0	—
	c.1512G>C	p.E504D	1 (SBA)	0	0	0	0	0	99%
	c.1519G>C	p.G507R	1 (An)	0	0	0	0	0	17%
	c.1525C>G	p.P509A[e]	1 (An)	0	0	0	0	0	41%
	c.1550G>C	p.S517T	0	0	0	0	1 (SBA)	0	—
	c.1570G>C	p.V524L	1 (SBA)	0	0	0	0	0	34%
Exon 14	c.1705G>A	p.A569T[f]	3 (SBA/SBO/SBO)	1	0	0	1 (SBA)	0	40%
Exon 17	c.1953T>C	p.H651H	0	1	0	0	0	—	—
Exon 19	c.2203G>T	p.V735L	0	2	0	0	0	—	81%
Intron 19	c.2316-1G>A	splice	1 (SBA)	0	0	0	0	—	
Exon 20	c.2380G>A	p.A794T	2 (SBASBA)	0	0	0	2 (SBA)	2	88%
	c.2406G>A	p.A802A	1 (An)	0	0	0	0	0	—
Exon 21	c.2474G>A	p.G825D	0	0	1 (An)	0	0	—	24%
	c.2487C>T	p.A829A	0	1	0	0	0	—	—
	c.2565A>C	p.A855A	1 (An)	0	0	0	0	—	—
Exon 23	c.2746C>T	p.L916L	1 (Crn)	0	0	0	0	—	—
Exon 25	c.2964G>A	p.R988R	0	0	0	0	1 (SBA)	0	—
	c.2965A>G	p.I989V	0	1	0	0	0	0	130%
GCSH									
Exon 1	c.53C>T	p.A18V	1 (An)	1	0	0	—	—	

All nucleotide changes were found in heterozygous form. One individual carried c.52G>T and c.1705G>A in *GLDC*, whereas no other individuals carried more than one of the nucleotide changes listed here. Eight silent polymorphisms and four missense variants present in dbSNP (http://www.ncbi.nlm.nih.gov/projects/SNP/) are not listed in this table and include: *AMT*: c.954G>A (p.R318R, rs11715915); *GLDC*: c.249G>A (p.G83G, rs12341698), c.438G>A (p.T146T, rs13289273), c.501G>A (p.E167E, rs13289273), c.660C>T (p.L220L, rs2228095), c.666T>C (p.D222D, rs12004164), c.671G>A (p.R224H, rs28617412) and c.1384C>G (p.L462V, rs73400312); and for *GCSH*: c.62T>C (p.S21L, rs8052579), c.90C>G (p.P30P, rs8177847), c.159C>T (p.F53F, rs177876), c.218A>G (N73S, rs8177876), c.252T>C (Y84Y, rs8177907) and c.261C>G (L87L, rs8177908). Grey shading indicates loss-of-function mutations, based on enzymatic activity in the *in vitro* expression study or splicing defect.

[a]Residual enzymatic activity of GLDC mutant protein is expressed as %activity of the wild-type enzyme (Fig. 2).

[b]SBA, spina bifida aperta; SBO, spina bifida occulta; An, anencephaly; Crn, craniorachischisis.

[c]Total number of UK, Japanese or Swedish NTD patients.

[d]This variant was previously established as likely to be a non-functional polymorphism by segregation in an NKH family (21).

[e]A biochemical test of folate metabolism, the dU suppression test, was previously performed on primary fibroblasts derived from this patient and showed a defect of thymidylate biosynthesis to be present (14).

[f]p.A569T has previously been reported as a pathogenic mutation in a patient with typical NKH (21).

In *AMT*, we identified two novel sequence variants predicted to result in non-synonymous missense changes, c.589G>C (D197H) and c.850G>C (V284L), in anencephaly and spina bifida patients, respectively, from the UK cohort (Table 1). Neither variant was present in 526 UK or 36 Japanese control subjects or in the SNP databases dbSNP and 1000 Genomes. An additional missense variant, E211K, was also identified in three spina bifida patients, two from the UK and one from Sweden. Causative mutations in *AMT* have been found previously in an autosomal recessive inborn error of metabolism, non-ketotic hyperglycaemia (NKH) (17). The E211K variant had previously been identified in an NKH family but was established as likely to be a non-functional polymorphism by segregation (21). Therefore, this variant is considered unlikely to be causally related to NTDs.

Exon sequencing of *GCSH* revealed eight single-base substitutions, one of which (c.53C>T, p.A18V) was a novel change found in both an NTD and a single control (Table 1). The others all corresponded to known SNPs, which did not suggest a role for *GCSH* in NTDs.

Next we turned our attention to *GLDC*, in which we identified 27 single-base substitutions (Table 1), including 11 silent nucleotide changes, 15 non-synonymous changes and a splicing acceptor variant of intron 19 (c.2316-1G>A). The

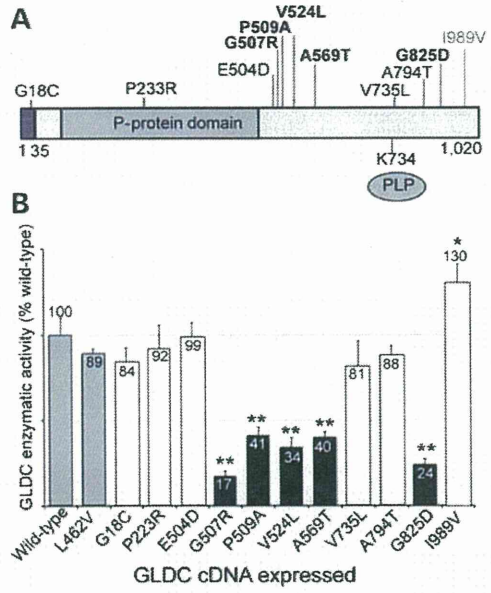

Figure 2. Characterization of *GLDC* missense mutations identified through DNA sequence analysis. (**A**) The schematic represents the 1020 amino acid residue GLDC polypeptide with the positions of the identified missense variants indicated. Mutations conferring significantly reduced activity (**B**) are indicated in bold. The leader peptide for mitochondrial import (shaded black) and the lysine 754-binding site for the co-factor pyridoxal phosphate (PLP) are indicated (49). (B) Enzymatic activity of GLDC missense variants. Expression vectors with wild-type and mutant *GLDC* cDNAs were transfected into COS7 cells for the evaluation of GLDC activity, which is expressed as relative activity (%) of cells expressing wild-type cDNA (shaded grey). The L462V GLDC enzyme (shaded grey) was tested as an example of a normally occurring variant (rs73400312). Variant proteins whose activities were significantly diminished compared with wild-type are indicated by black shading. The I989V variant, identified in a control parent, showed significantly elevated activity. Values are given as mean ± SD of triplicate experiments ($^{*}P < 0.05$; $^{**}P < 0.01$, compared with wild-type).

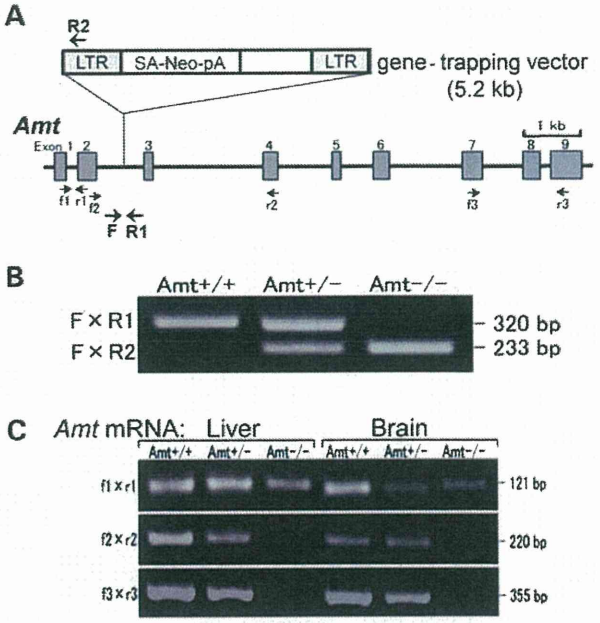

Figure 3. Generation of *Amt* knockout mouse by gene trapping. (**A**) The location of the gene-trap vector in *Amt* intron 2 in the ES cell line OST181110 was determined by inverse PCR. Mice carrying this mutation were generated using standard methods of blastocyst microinjection with OST181110 ES cells to generate chimeras, and germ-line transmission. LTR, long terminal repeats; SA, splicing acceptor site; Neo, neomycin phosphotransferase gene; pA, polyadenylation sequence. (**B**) For genotyping, mouse genomic DNA was subjected to allele-specific amplification with F, R1 and R2 primers (Supplementary Material, Table S1). A genomic fragment of 320 bp was amplified from the wild-type allele, whereas a 233 bp fragment was amplified from the *Amt*-mutant allele. (**C**) RT-PCR analysis of *Amt* mRNA expressed in the brain and liver of *Amt*-mutant mice. Primers in exon 1–2 generated a 121 bp band irrespective of mouse genotypes. RT-PCR in which either one (f2-r2) or both (f3-r3) primers were located in exons 3′ to the insertion site produced 220 and 355 bp cDNA fragments, respectively, in $Amt^{+/+}$ and $Amt^{+/-}$ mice, but not in $Amt^{-/-}$. The *Amt* mRNA in mice carrying the trap vector was, therefore, aberrantly spliced at the end of exon 2, resulting in truncation of *Amt* mRNA in $Amt^{-/-}$ mice.

latter is deduced to abolish normal splicing of the *GLDC* mRNA, with predicted skipping of exon 19 resulting in loss of the reading frame. Among the 15 missense variants identified in *GLDC*, 5 were unique to the NTD group, being absent from all 562 control individuals as well as from the SNP databases. A further three novel variants were found only in controls, whereas the remainder were found in both NTDs and controls, and included previously reported SNPs.

We investigated the possible functional effects of *GLDC* missense variants by expressing wild-type and mutant cDNA constructs in COS7 cells, followed by enzymatic assay of GLDC activity involving a decarboxylation reaction using [1-^{14}C]glycine (22). Twelve GLDC variants were tested, including those that were unique to NTD patients and, therefore, hypothesized to be potentially pathogenic (Fig. 2). The L462V variant, which corresponds to a known SNP (rs73400312), was included as an example of a known normally occurring form. Five of the missense changes, G507R, P509A, V524L, A569T and G825D, resulted in a significant reduction in GLDC activity compared with the wild-type protein ($P < 0.001$). Notably, all five of these deleterious variants were present solely in NTD cases, whereas none of the variants that were unique to controls (P223R, V735L and I989V) showed loss of enzymatic function. In the case of G18C and A794T, which occurred in both NTDs and controls, there was no significant loss of enzymatic activity, suggesting that these are unlikely to be causative mutations.

Having identified putative mutations in *AMT* and *GLDC* in NTD patients, we hypothesized that loss of GCS function could predispose to development of NTDs. In order to directly test the functional requirement for GCS activity in neural tube closure, we generated mice that lacked GCS activity, using a gene trap (OmniBank, OST181110) of the *Amt* gene. The vector was located in intron 2, resulting in a truncated transcript that lacked exons 3–9 (Fig. 3). The efficacy of the gene-trap vector in trapping expression of *Amt* (Amt^{-}) was confirmed by RT-PCR analysis (Fig. 3). Heterozygous $Amt^{+/-}$ mice were viable and fertile and exhibited no obvious malformations. Homozygous $Amt^{-/-}$ mice were not observed among post-natal litters from heterozygote intercrosses, and so fetuses were examined at embryonic day (E) 17.5. Strikingly, 87% of $Amt^{-/-}$ fetuses (34 out of 39) exhibited NTDs, whereas no malformations were observed in $Amt^{+/+}$ ($n = 33$) or $Amt^{+/-}$

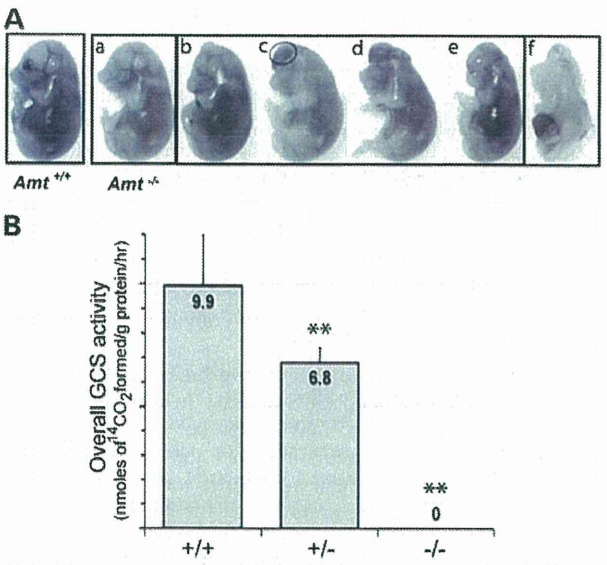

Figure 4. Mice lacking GCS activity exhibit NTDs. (**A**) Phenotypes of *Amt* mutant mice. NTDs were evident in the majority (88%) of $Amt^{-/-}$ fetuses (examples shown are at E17.5). Various types of NTDs were observed in $Amt^{-/-}$ fetuses, which principally affected the cranial region; a, no NTDs; b, small exencephaly (dotted circle); c–e, large exencephaly; f, craniorachischisis. (**B**) Enzymatic activity of the GCS in *Amt* knockout mice. $Amt^{+/-}$ and $Amt^{-/-}$ fetuses had significantly lower GCS activity in the liver than $Amt^{+/+}$ fetuses, with activity in $Amt^{-/-}$ samples below the level of detection ($^{**}P < 0.01$ compared with $Amt^{+/+}$).

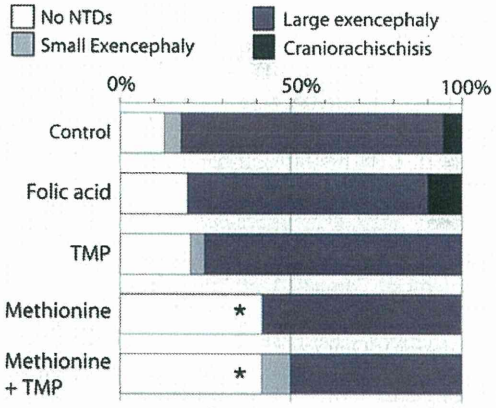

Figure 5. Maternal supplementation of *Amt* mutant embryos with folic acid, TMP or methionine. Maternal treatment with folic acid ($n = 10$ homozygous mutant fetuses) or TMP ($n = 12$) had no significant effect on NTD frequency, whereas the frequency of unaffected embryos was significantly increased following treatment with methionine ($n = 12$) or methionine plus TMP group ($n = 12$). The asterisk indicates significant difference compared with non-treated group ($P < 0.05$).

($n = 66$) fetuses. Defects mainly comprised exencephaly (82%), in which the cranial neural folds persistently failed to close (Fig. 4). There was also a low frequency of the more severe condition, craniorachischisis (5%), in which the neural tube remains open from the mid- and hindbrain, and throughout the spinal region (Fig. 4). Fetal liver samples were subjected to enzyme assay to determine overall activity of the GCS. In $Amt^{-/-}$ mice, overall GCS activity was effectively ablated being below the detection level of the assay (0.01 nmoles of $^{14}CO_2$ formed/gram protein/h), consistent with the Amt^{-} allele being a functional null (22) (Fig. 4). These findings confirm that AMT function is essential for GCS activity, and that the latter is necessary for successful neural tube closure.

Given that GCS is a component of FOCM (Fig. 1), we evaluated the possible prevention of NTDs by folate-related metabolites. Maternal supplementation was performed with folic acid, thymidine monophosphate (TMP), methionine or methionine plus TMP (23). Neither folic acid nor TMP significantly affected the frequency of NTDs among the homozygous $Amt^{-/-}$ offspring. However, we observed a significant protective effect of maternal supplementation with methionine or methionine plus TMP, compared with the non-treated group ($P < 0.05$; Fig. 5).

DISCUSSION

NTDs remain among the commonest human birth defects and understanding their genetic basis presents a considerable challenge owing to their multigenic inheritance and the potential influence of environmental factors, either predisposing or ameliorating. Several lines of evidence indicate a requirement for FOCM in neural tube closure and, therefore, GCS-encoding genes provide excellent candidates for possible involvement in NTD susceptibility. We identified putative mutations in *AMT* and *GLDC* which include a splice acceptor mutation and a number of non-synonymous variants that were absent from a large group of population-matched controls, as well as from public SNP databases. In the case of *GLDC*, enzymatic assay confirmed that several mutations resulted in significant loss of enzyme activity. Finally, *in vivo* functional evidence of a requirement for GCS function in neural tube closure was provided by the occurrence of NTDs in $Amt^{-/-}$ mice lacking GCS activity. Together these findings indicate that mutations in *GLDC* and *AMT* predispose to NTDs in both mice and humans.

Where parental samples were available (6 of the 11 NTD cases that involved putative mutations in *GLDC*), we demonstrated parent-to-child transmission (Supplementary Material, Table S2). Six were instances of maternal transmission and one involved paternal transmission. We hypothesize that absence of an overt NTD phenotype in parents who carry a deficient *GLDC* allele may result from incomplete penetrance, or lack of additional genetic or environmental factors which are predicted to be necessary for NTDs owing to their multifactorial aetiology. We also note that partial penetrance is a feature of numerous mouse models of NTDs (5,8).

Inherited GCS deficiency, owing to mutation of *AMT* and/or *GLDC*, has been shown to cause NKH in humans (17). NKH is a rare, autosomal recessive, inborn error of metabolism, characterized by accumulation of glycine and encephalopathy-like neurological signs, including coma and convulsive seizures in neonates. GCS activity is greatly diminished in NKH patients and they would, therefore, be predicted to be at increased risk of NTDs. It is possible that NTDs may occur in combination with NKH but as anencephaly is a lethal condition, co-existing

NKH would go undetected. Lack of NTDs in NKH patients may also reflect the multigenic nature of NTDs, which require the presence of additional risk alleles in non-GCS genes. NKH is a relatively rare condition, with a prevalence of 1/63 000 births in British Columbia (24) and 1/250 000 in the USA (25). It is therefore possible that an increased risk of NTDs among carriers of GCS mutations in NKH families may not have been noted and this possibility is worthy of investigation. Based on estimated carrier frequency and the incidence of mutations among NTD patients, we predict that NTDs might be expected among 1/150 of the siblings of NKH patients (see Supplementary Material, Table S3 for estimate calculation). One case report of an NKH patient with a *GLDC* mutation describes the additional presence of spinal cord hydromyelia (19). This condition is often associated with low spinal defects (involving secondary neurulation), but it is also possible that the expanded spinal canal was also present at a higher level and might indicate a limited defect in primary neurulation.

The mutations described in the current study were all present in heterozygous form and, therefore, are hypothesized to be insufficient to cause NKH while predisposing to NTDs. For example, in the current study we found four NTD patients and one control individual to be heterozygous for the A569T mutation, which is shown to result in reduced enzyme activity. This mutation was previously identified in a Caucasian patient with typical NKH, in combination with a second mutation, P765S (26), confirming that it is deleterious *in vivo*. Hence, we predict that, depending on the co-existing genetic milieu, the A569T variant may cause NKH, predispose to NTDs or be compatible with normal development.

The high incidence of NTDs in *AMT* mutant mice is particularly notable as NTDs have not previously been found to be a common feature of mouse models deficient for folate-metabolizing enzymes. This includes null mutants that have been reported for eight other genes that encode enzymes in FOCM (Fig. 1A) (27). Four have normal morphology at birth (*Cbs*, *Mthfd1*, *Mthfr* and *Shmt1*) (28–31), *Mthfd2* null embryos die by E15.5 but neural tube closure is complete (32) and null mutants for *Mtr*, *Mtrr* and *Mthfs* die before E9.5, prior to neural tube closure (33–35). Although analysis of mouse mutants has not supported a role for single-gene mutations in FOCM as major causes of NTDs, a requirement for cellular uptake of folate for neural tube closure has been demonstrated in *Folr1* null embryos, in which NTDs occur when rescued from early lethality by folic acid supplementation (36). There is also considerable evidence for possible involvement of gene–environment and/or gene–gene interactions in NTDs. For example, in *Pax3* mutant (*splotch*) embryos, which exhibit a defect of thymidylate biosynthesis, dietary folate-deficiency increases the frequency of cranial NTDs (23,37). Similarly, a diet deficient in folate and choline causes NTDs in *Shmt1* mutant embryos, whereas *Shmt1* and *Pax3* mutations exhibit genetic interaction (38).

Regarding the mechanisms by which GCS mutations affect neural tube closure, a key question is whether NTDs are caused by impairment of FOCM or by another cause such as glycine accumulation. Modelling of hepatic FOCM, based on biochemical properties of folate-metabolizing enzymes (39), predicts that loss of the mitochondrial GCS reaction would reduce the efflux rate of formate to the cytosol by ~50%. This results in reduced synthesis of purines and thymidylate, which are essential for the rapid cell division in the closing neural folds. Interestingly, a UK patient with anencephaly who was found to carry the *GLDC* loss-of-function mutation P509A in the current study (Table 1) was previously found to have impaired thymidylate biosynthesis, assayed in cultured fibroblasts (14). These findings support the hypothetical link between diminished GLDC function, reduced thymidylate biosynthesis and development of NTDs. Reduced thymidylate biosynthesis and diminished cellular proliferation are proposed to underlie folate-related cranial NTDs in *splotch* (*Pax3*) mouse mutants (37,38).

As well as impairment of nucleotide biosynthesis, the predicted effect of diminished GCS activity in reducing production of methionine (39) may also be of relevance as methionine is the precursor for the methyl donor *S*-adenosylmethionine. Indeed, metabolic tracing experiments suggest that ~80% of 1C units in the methylation cycle are generated within mitochondrial FOCM (40). Impairment of the methylation cycle and/or DNA methylation is known to cause NTDs in mice (41) and is proposed as a possible cause of human NTDs (7,42). It was therefore notable that we found a preventive effect of methionine supplementation in $Amt^{-/-}$ mice. Together, these findings suggest that FOCM, required for both thymidylate biosynthesis and methylation reactions that are essential for neural tube closure, may be functionally deficient in individuals who have mutations in *GLDC* or *AMT*.

MATERIALS AND METHODS

Patient cohorts and sequencing

Mutation analysis by DNA sequencing was performed on all exons of *AMT*, *GCSH* and *GLDC* as described (26). Cases comprised Japanese patients with anencephaly ($n = 14$) and two separate cohorts of UK patients with a diagnosis of anencephaly (combined $n = 24$), spina bifida ($n = 122$) or craniorachischisis ($n = 22$). In addition, the exons of *AMT*, *GCSH* and *GLDC* were sequenced in 76 Swedish patients with spina bifida. Unaffected controls, completely sequenced for these genes, comprised 36 Japanese and 189 unrelated UK subjects. Exons found to contain missense mutations were also sequenced in a further cohort of 192 well-characterized UK controls (43) and in 145 Swedish controls. This study was approved by the Ethical Committees of Tohoku University School of Medicine, UCL Institute of Child Health, Newcastle University and the Karolinska Institute.

Enzymatic assay of GCS activity and GLDC activity

GCS activity was measured in mouse liver samples by a decarboxylation reaction using [1-^{14}C]glycine as described (22). For analysis of GLDC activity, wild-type and mutant *GLDC* cDNAs were cloned into pCAG expression vector, kindly provided by Professor Jun-ichi Miyazaki (Osaka University, Japan) (44). Constructs were transfected into COS7 cells, which were harvested as described previously and cell pellets stored at −80°C prior to analysis (45). GLDC

enzymatic activity was determined, in triplicate, by exchange reaction between carbon dioxide and glycine using $NaH^{14}CO_3$ in the presence of excess recombinant bovine GCSH protein as described (22). An expression system of lipoylated bovine GCSH protein in *Escherichia coli* was kindly provided by Dr Kazuko Fujiwara (Tokushima University, Japan) (46). Statistical analysis was performed using SPSS software version 11.0 (SPSS, Inc., Chicago, IL, USA).

Knockout of Amt by insertion of a gene-trap vector

Mice carrying a gene-trap allele of *Amt* (here denoted Amt^{-}) were generated at Lexicon Genetics, Inc. (Houston, TX, USA) using the OST181110 ES cell line. The genomic insertion site of the gene-trap vector was determined by inverse PCR and localized to intron 2 (Supplementary Material, Fig. S1). Total RNA was prepared from the mouse liver and brain at E18 for RT-PCR analysis (Supplementary Material, Fig. S1 and Table S1). $Amt^{+/-}$ mice were backcrossed with wild-type C57BL/6 mice for nine generations to generate a congenic line of mice on the C57BL/6 background, for use in biochemical and histological analyses. This study was approved by the Animal Experiment Committee of Tohoku University.

Maternal supplementation with folic acid and related metabolites

Dams were treated with folic acid (25 mg/kg), thymidine-1-phosphate (TMP; 30 mg/kg) or L-methionine (70 mg/kg) by intra-peritoneal injection, 2 h prior to mating and daily from E7.5–10.5. Doses were based on previous studies (23,47,48).

SUPPLEMENTARY MATERIAL

Supplementary Material is available at *HMG* online.

Conflict of Interest statement. None declared.

FUNDING

This work was supported by a research grant from the Ministry of Education, Culture, Sports, Science and Technology and a Research Grant from the Ministry of Health, Labour and Public Welfare in Japan. Research at Newcastle University was funded by the Newlife Foundation. Research at UCL Institute of Child Health was supported by SPARKS, the Wellcome Trust, Medical Research Council, UCL Biomedical Research Centre and by Great Ormond Street Hospital Children's Charity. Funding to pay the Open Access publication charges for this article was provided by the Wellcome Trust.

REFERENCES

1. Greene, N.D. and Copp, A.J. (2009) Development of the vertebrate central nervous system: formation of the neural tube. *Prenatal Diag.*, **29**, 303–311.
2. Harris, M.J. and Juriloff, D.M. (2007) Mouse mutants with neural tube closure defects and their role in understanding human neural tube defects. *Birth Defects Res. A Clin. Mol. Teratol.*, **79**, 187–210.
3. Greene, N.D.E., Stanier, P. and Copp, A.J. (2009) Genetics of human neural tube defects. *Hum. Mol. Genet.*, **18**, R113–R129.
4. Au, K.S., Ashley-Koch, A. and Northrup, H. (2010) Epidemiologic and genetic aspects of spina bifida and other neural tube defects. *Dev. Disabil. Res. Rev.*, **16**, 6–15.
5. Harris, M.J. and Juriloff, D.M. (2010) An update to the list of mouse mutants with neural tube closure defects and advances toward a complete genetic perspective of neural tube closure. *Birth Defects Res. A Clin. Mol. Teratol.*, **88**, 653–669.
6. Copp, A.J. and Greene, N.D.E. (2010) Genetics and development of neural tube defects. *J. Pathol.*, **220**, 217–230.
7. Blom, H.J., Shaw, G.M., Den Heijer, M. and Finnell, R.H. (2006) Neural tube defects and folate: case far from closed. *Nat. Rev. Neurosci.*, **7**, 724–731.
8. Molloy, A.M., Brody, L.C., Mills, J.L., Scott, J.M. and Kirke, P.N. (2009) The search for genetic polymorphisms in the homocysteine/folate pathway that contribute to the etiology of human neural tube defects. *Birth Defects Res. A Clin. Mol. Teratol.*, **85**, 285–294.
9. Beaudin, A.E. and Stover, P.J. (2009) Insights into metabolic mechanisms underlying folate-responsive neural tube defects: a mini review. *Birth Defects Res. A Clin. Mol. Teratol.*, **85**, 274–284.
10. Tibbetts, A.S. and Appling, D.R. (2010) Compartmentalization of mammalian folate-mediated one-carbon metabolism. *Annu. Rev. Nutr.*, **30**, 57–81.
11. Boyles, A.L., Hammock, P. and Speer, M.C. (2005) Candidate gene analysis in human neural tube defects. *Am. J. Med. Genet. C Semin. Med. Genet.*, **135**, 9–23.
12. Shaw, G.M., Lu, W., Zhu, H., Yang, W., Briggs, F.B., Carmichael, S.L., Barcellos, L.F., Lammer, E.J. and Finnell, R.H. (2009) 118 SNPs of folate-related genes and risks of spina bifida and conotruncal heart defects. *BMC Med. Genet.*, **10**, 49.
13. Martinez, C.A., Northrup, H., Lin, J.I., Morrison, A.C., Fletcher, J.M., Tyerman, G.H. and Au, K.S. (2009) Genetic association study of putative functional single nucleotide polymorphisms of genes in folate metabolism and spina bifida. *Am. J. Obstet. Gynecol.*, **201**, 394–411.
14. Dunlevy, L.P.E., Chitty, L.S., Doudney, K., Burren, K.A., Stojilkovic-Mikic, T., Stanier, P., Scott, R., Copp, A.J. and Greene, N.D.E. (2007) Abnormal folate metabolism in foetuses affected by neural tube defects. *Brain*, **130**, 1043–1049.
15. Parle-McDermott, A., Pangilinan, F., O'Brien, K.K., Mills, J.L., Magee, A.M., Troendle, J., Sutton, M., Scott, J.M., Kirke, P.N., Molloy, A.M. and Brody, L.C. (2009) A common variant in MTHFD1L is associated with neural tube defects and mRNA splicing efficiency. *Hum. Mutat.*, **30**, 1650–1656.
16. Kikuchi, G. (1973) The glycine cleavage system: composition, reaction mechanism, and physiological significance. *Mol. Cell. Biochem.*, **1**, 169–187.
17. Kure, S., Tada, K. and Narisawa, K. (1997) Nonketotic hyperglycinemia: biochemical, molecular, and neurological aspects. *Jpn J. Hum. Genet*, **42**, 13–22.
18. Kure, S., Narisawa, K. and Tada, K. (1992) Enzymatic diagnosis of nonketotic hyperglycinemia with lymphoblasts. *J. Pediatr.*, **120**, 95–98.
19. Hayasaka, K., Tada, K., Kikuchi, G., Winter, S. and Nyhan, W.L. (1983) Nonketotic hyperglycinemia: two patients with primary defects of P-protein and T-protein, respectively, in the glycine cleavage system. *Pediatr. Res.*, **17**, 967–970.
20. Ichinohe, A., Kure, S., Mikawa, S., Ueki, T., Kojima, K., Fujiwara, K., Iinuma, K., Matsubara, Y. and Sato, K. (2004) Glycine cleavage system in neurogenic regions. *Eur. J. Neurosci.*, **19**, 2365–2370.
21. Toone, J.R., Applegarth, D.A., Kure, S., Coulter-Mackie, M.B., Sazegar, P., Kojima, K. and Ichinohe, A. (2002) Novel mutations in the P-protein (glycine decarboxylase) gene in patients with glycine encephalopathy (non-ketotic hyperglycinemia). *Mol. Genet. Metab.*, **76**, 243–249.
22. Sakata, Y., Owada, Y., Sato, K., Kojima, K., Hisanaga, K., Shinka, T., Suzuki, Y., Aoki, Y., Satoh, J., Kondo, H. *et al.* (2001) Structure and expression of the glycine cleavage system in rat central nervous system. *Brain Res. Mol. Brain Res.*, **94**, 119–130.
23. Fleming, A. and Copp, A.J. (1998) Embryonic folate metabolism and mouse neural tube defects. *Science*, **280**, 2107–2109.

24. Applegarth, D.A., Toone, J.R. and Lowry, R.B. (2000) Incidence of inborn errors of metabolism in British Columbia, 1969–1996. *Pediatrics*, **105**, e10.
25. Nyhan, W.L. (1989) Nonketotic hyperglycinemia. In Scriver, C.R., Beaudet, A.L., Sly, W.S. and Valle, D. (eds), *The Metabolic Basis of Inherited Disease*. McGraw-Hill, Inc., New York, 743–753.
26. Kure, S., Kato, K., Dinopoulos, A., Gail, C., DeGrauw, T.J., Christodoulou, J., Bzduch, V., Kalmanchey, R., Fekete, G., Trojovsky, A. *et al.* (2006) Comprehensive mutation analysis of GLDC, AMT, and GCSH in nonketotic hyperglycinemia. *Hum. Mutat.*, **27**, 343–352.
27. Harris, M.J. (2008) Insights into prevention of human neural tube defects by folic acid arising from consideration of mouse mutants. *Birth Defects Res. A Clin. Mol. Teratol.*, **85**, 331–339.
28. Watanabe, M., Osada, J., Aratani, Y., Kluckman, K., Reddick, R., Malinow, M.R. and Maeda, N. (1995) Mice deficient in cystathionine β-synthase: animal models for mild and severe homocyst(e)inemia. *Proc. Natl Acad. Sci. USA*, **92**, 1585–1589.
29. Champion, K.M., Cook, R.J., Tollaksen, S.L. and Giometti, C.S. (1994) Identification of a heritable deficiency of the folate-dependent enzyme 10-formyltetrahydrofolate dehydrogenase in mice. *Proc. Natl Acad. Sci. USA*, **91**, 11338–11342.
30. Chen, Z., Karaplis, A.C., Ackerman, S.L., Pogribny, I.P., Melnyk, S., Lussier-Cacan, S., Chen, M.F., Pai, A., John, S.W., Smith, R.S. *et al.* (2001) Mice deficient in methylenetetrahydrofolate reductase exhibit hyperhomocysteinemia and decreased methylation capacity, with neuropathology and aortic lipid deposition. *Hum. Mol. Genet.*, **10**, 433–443.
31. MacFarlane, A.J., Liu, X., Perry, C.A., Flodby, P., Allen, R.H., Stabler, S.P. and Stover, P.J. (2008) Cytoplasmic serine hydroxymethyltransferase regulates the metabolic partitioning of methylenetetrahydrofolate but is not essential in mice. *J. Biol. Chem.*, **283**, 25846–25853.
32. Di, P.E., Sirois, J., Tremblay, M.L. and Mackenzie, R.E. (2002) Mitochondrial NAD-dependent methylenetetrahydrofolate dehydrogenase-methenyltetrahydrofolate cyclohydrolase is essential for embryonic development. *Mol. Cell. Biol.*, **22**, 4158–4166.
33. Swanson, D.A., Liu, M.L., Baker, P.J., Garrett, L., Stitzel, M., Wu, J.M., Harris, M., Banerjee, R., Shane, B. and Brody, L.C. (2001) Targeted disruption of the methionine synthase gene in mice. *Mol. Cell. Biol.*, **21**, 1058–1065.
34. Elmore, C.L., Wu, X., Leclerc, D., Watson, E.D., Bottiglieri, T., Krupenko, N.I., Krupenko, S.A., Cross, J.C., Rozen, R., Gravel, R.A. and Matthews, R.G. (2007) Metabolic derangement of methionine and folate metabolism in mice deficient in methionine synthase reductase. *Mol. Genet. Metab.*, **91**, 85–97.
35. Field, M.S., Anderson, D.D. and Stover, P.J. Mthfs is an essential gene in mice and a component of the purinosome. *Front. Genet.* http://www.frontiersin.org/nutrigenomics/10.3389/fgene.2011.00036/abstract.
36. Spiegelstein, O., Mitchell, L.E., Merriweather, M.Y., Wicker, N.J., Zhang, Q., Lammer, E.J. and Finnell, R.H. (2004) Embryonic development of folate binding protein-1 (Folbp1) knockout mice: effects of the chemical form, dose, and timing of maternal folate supplementation. *Dev. Dyn.*, **231**, 221–231.
37. Burren, K.A., Savery, D., Massa, V., Kok, R.M., Scott, J.M., Blom, H.J., Copp, A.J. and Greene, N.D.E. (2008) Gene-environment interactions in the causation of neural tube defects: folate deficiency increases susceptibility conferred by loss of *Pax3* function. *Hum. Mol. Genet.*, **17**, 3675–3685.
38. Beaudin, A.E., Abarinov, E.V., Noden, D.M., Perry, C.A., Chu, S., Stabler, S.P., Allen, R.H. and Stover, P.J. (2011) Shmt1 and de novo thymidylate biosynthesis underlie folate-responsive neural tube defects in mice. *Am. J. Clin. Nutr.*, **93**, 789–798.
39. Nijhout, H.F., Reed, M.C., Lam, S.L., Shane, B., Gregory, J.F. III and Ulrich, C.M. (2006) In silico experimentation with a model of hepatic mitochondrial folate metabolism. *Theor. Biol. Med. Model.*, **3**, 40.
40. Pike, S.T., Rajendra, R., Artzt, K. and Appling, D.R. (2010) Mitochondrial C1-tetrahydrofolate synthase (MTHFD1L) supports the flow of mitochondrial one-carbon units into the methyl cycle in embryos. *J. Biol. Chem.*, **285**, 4612–4620.
41. Dunlevy, L.P.E., Burren, K.A., Mills, K., Chitty, L.S., Copp, A.J. and Greene, N.D.E. (2006) Integrity of the methylation cycle is essential for mammalian neural tube closure. *Birth Defects Res. A*, **76**, 544–552.
42. Greene, N.D., Stanier, P. and Moore, G.E. (2011) The emerging role of epigenetic mechanisms in the aetiology of neural tube defects. *Epigenetics*, **6**, 875–893.
43. Apostolidou, S., Abu-Amero, S., O'Donoghue, K., Frost, J., Olafsdottir, O., Chavele, K.M., Whittaker, J.C., Loughna, P., Stanier, P. and Moore, G.E. (2007) Elevated placental expression of the imprinted PHLDA2 gene is associated with low birth weight. *J. Mol. Med.*, **85**, 379–387.
44. Niwa, H., Yamamura, K. and Miyazaki, J. (1991) Efficient selection for high-expression transfectants with a novel eukaryotic vector. *Gene*, **108**, 193–199.
45. Oda, M., Kure, S., Sugawara, T., Yamaguchi, S., Kojima, K., Shinka, T., Sato, K., Narisawa, A., Aoki, Y., Matsubara, Y. *et al.* (2007) Direct correlation between ischemic injury and extracellular glycine concentration in mice with genetically altered activities of the glycine cleavage multienzyme system. *Stroke*, **38**, 2157–2164.
46. Fujiwara, K., Okamura-Ikeda, K. and Motokawa, Y. (1991) Lipoylation of H-protein of the glycine cleavage system. The effect of site-directed mutagenesis of amino acid residues around the lipoyllysine residue on the lipoate attachment. *FEBS Lett.*, **293**, 115–118.
47. Wlodarczyk, B.J., Tang, L.S., Triplett, A., Aleman, F. and Finnell, R.H. (2006) Spontaneous neural tube defects in splotch mice supplemented with selected micronutrients. *Toxicol. Appl. Pharmacol.*, **213**, 55–63.
48. Essien, F.B. and Wannberg, S.L. (1993) Methionine but not folinic acid or vitamin B-12 alters the frequency of neural tube defects in *Axd* mutant mice. *J. Nutr.*, **123**, 27–34.
49. Nakai, T., Nakagawa, N., Maoka, N., Masui, R., Kuramitsu, S. and Kamiya, N. (2005) Structure of P-protein of the glycine cleavage system: implications for nonketotic hyperglycinemia. *EMBO J.*, **24**, 1523–1536.

PEDIATRICS INTERNATIONAL Official Journal of the Japan Pediatric Society

Pediatrics International (2011) **53**, 921–925 doi: 10.1111/j.1442-200X.2011.03412.x

Original Article

Neonatal lactic acidosis with methylmalonic aciduria due to novel mutations in the *SUCLG1* gene

Osamu Sakamoto,[1] Toshihiro Ohura,[1,2] Kei Murayama,[5] Akira Ohtake,[6] Hiroko Harashima,[6] Daiki Abukawa,[3] Junji Takeyama,[4] Kazuhiro Haginoya,[1] Shigeaki Miyabayashi[1] and Shigeo Kure[1]

[1]*Department of Pediatrics, Tohoku University School of Medicine,* [2]*Department of Pediatrics, Sendai City Hospital, Departments of* [3]*General Pediatrics and* [4]*Pathology, Miyagi Children's Hospital, Sendai,* [5]*Department of Metabolism, Chiba Children's Hospital, Chiba and* [6]*Department of Pediatrics, Faculty of Medicine, Saitama Medical University, Saitama, Japan*

Abstract ***Background***: Succinyl-coenzyme A ligase (SUCL) is a mitochondrial enzyme that catalyses the reversible conversion of succinyl-coenzyme A to succinate. SUCL consists of an α subunit, encoded by *SUCLG1*, and a β subunit, encoded by either *SUCLA2* or *SUCLG2*. Recently, mutations in *SUCLG1* or *SUCLA2* have been identified in patients with infantile lactic acidosis showing elevated urinary excretion of methylmalonate, mitochondrial respiratory chain (MRC) deficiency, and mitochondrial DNA depletion.

Methods: Case description of a Japanese female patient who manifested a neonatal-onset lactic acidosis with urinary excretion of methylmalonic acid. Enzymatic analyses (MRC enzyme assay and Western blotting) and direct sequencing analysis of *SUCLA2* and *SUCLG1* were performed.

Results: MRC enzyme assay and Western blotting showed that MRC complex I was deficient. *SUCLG1* mutation analysis showed that the patient was a compound heterozygote for disease-causing mutations (p.M14T and p.S200F).

Conclusion: For patients showing neonatal lactic acidosis and prolonged mild methylmalonic aciduria, MRC activities and mutations of *SUCLG1* or *SUCLA2* should be screened for.

Key words lactic acidosis, methylmalonic acid, mitochondrial respiratory chain, *SUCLA2*, *SUCLG1*.

Urinary excretion of methylmalonic acid is caused by a defect in the isomerization of L-methylmalonyl-coenzyme A to succinyl-coenzyme A. The reaction is catalyzed by L-methylmalonyl-coenzyme A mutase (MCM), an enzyme that requires adenosylcobalamin as a cofactor.[1] Methylmalonic acidemia/aciduria is mainly classified into two types: one resulting from a defect in the MCM apoenzyme and another resulting from a defect in the steps leading to adenosylcobalamin synthesis. In some cases, other causes of methylmalonic acidemia/aciduria have been reported. Recently, deficiency of the succinyl-coenzyme A ligase (SUCL) has been reported in cases of infantile lactic acidosis with mild urinary excretion of methylmalonic acid.[2]

Succinyl-coenzyme A ligase is a mitochondrial enzyme associated with the Krebs cycle, catalyzing the reversible conversion of succinyl-coenzyme A to succinate. The enzyme consists of two subunits. The substrate specificity for guanosine diphosphate (GDP) or adenosine diphosphate (ADP) is determined by the β subunit. The α subunit is encoded by the *SUCLG1* gene, whereas the β subunit is encoded by *SUCLA2* for the ADP-specific subunit and by *SUCLG2* for the GDP-specific subunit. *SUCLG1* is ubiquitously expressed, but its expression is particularly high in the heart, brain, kidney, and liver. The SUCLA2 protein is primarily present in the brain, skeletal muscle, and heart, and the SUCLG2 protein is present in the liver and kidney. More than 20 cases of deficiency in the α subunit (mutation in *SUCLG1*) or ADP-forming β subunit (mutation in *SUCLA2*) have been reported.[3–5] These patients have mitochondrial respiratory chain (MRC) deficiency, mitochondrial DNA (mtDNA) depletion, encephalomyopathy, and mild methylmalonic aciduria.[6–9]

Here, we describe the case of a Japanese female patient who presented with neonatal-onset lactic acidosis with urinary excretion of methylmalonic acid. *SUCLG1* mutation analysis showed that the patient was a compound heterozygote for disease-causing mutations.

Case report

In 1993 a female infant was born at 38 weeks gestation (birthweight, 2640 g; birth length, 47.3 cm). Her Apgar scores were normal. On the day after birth, she developed problems. Her blood sugar was lower than 1.1 mmol/L, and hence, continuous glucose infusion was started. Mechanical ventilation and peritoneal dialysis were started when the infant was 2 days old because of cyanosis, severe metabolic acidosis (pH, 6.638, base excess,

Correspondence: Osamu Sakamoto, MD, PhD, Department of Pediatrics, Tohoku University School of Medicine, 1-1 Seiryo-machi, Aoba-ku, Sendai 980-8574, Japan. Email: osakamoto-thk@umin.ac.jp

Received 15 December 2010; revised 23 April 2011; accepted 11 May 2011.

Table 1 Laboratory data

	2 days	4 days	4 months
WBC (/μL)	46 500	19 400	
RBC ($\times 10^6$/μL)	4.50	4.59	
Hb (g/dL)	18.0	18.0	
Ht (%)	59.0	51.5	
Plt ($\times 10^3$/μL)		105	
Total bilirubin (mg/dL)		8.8	
γ-GTP (IU/L)		136	
AST (IU/L)	607	217	
ALT (IU/L)	125	128	
LDH (IU/L)	5400	3860	
CK (IU/L)		6370	
CK-MB (IU/L)		216	
Na (mBq/L)		140	
K (mBq/L)		3.0	
TP (mg/dL)		4.7	
BUN (mg/dL)	23	24	
Cr (mg/dL)		1.2	
pH	6.638	7.477	
HCO_3^- (mEq/L)		14.5	
Base excess	−26.8	−4.9	
NH_3 (mmol/L)	191	45	
Lactate (mmol/L)	11	8.1	
Pyruvate (mmol/L)		0.41	
BS (mg/dL)		101	
Urine (organic acids excretion)		High, lactate, pyruvate; Moderate, methylmalonate, methylcitrate; Slight, glutarate, fumarate, succinate, 3-methylglutaconate	
Acylcarnitine (dried blood spots)			increase in C3 and C4DC
Methylmalonic acid (serum)			13 μmol/L (control, not detected MCM-deficient patients, 220–2900)
Methylmalonic acid (urine)			321 mmol/molCr (control, mean [SD], 2.0 [1.2])
^{14}C-propionate fixation (cultured fibroblasts)			8% of control

ALT, alanine aminotransferase; AST. aspartate aminotransferase; BS, blood sugar; BUN, blood urea nitrogen; CK, creatine kinase; γ-GTP, γ-glutamyltransferase; Hb, hemoglobin; Ht, hematocrit; LDH, lactate dehydrogenase; MCM, L-methylmalonyl-coenzyme A mutase; Plt, platelets; RBC, red blood cells; TP, total protein; WBC, white blood cells.

−26.8), lactic acidemia (11 mmol/L), and hyperammonemia (191 μmol/L; Table 1). She was transferred to Tohoku University Hospital at 4 days old.

Upon admission there was a swelling in the liver 4 cm below the costal margin. The lactate and pyruvate levels were 8.1 mmol/L and 0.41 mmol/L, respectively (L/P ratio, 20). Gas chromatography and mass spectrometry of urinary organic acid showed high levels of lactate and pyruvate excretion; moderate methylmalonate and methylcitrate excretion; and slight glutarate, fumarate, succinate, and 3-methylglutaconate excretion.

Acidosis improved on the following day, and mechanical ventilation and peritoneal dialysis were stopped. She developed prolonged hypotonia. At 1 month of age, auditory brainstem response was absent, and severe hearing impairment was noted. Head computed tomography showed diffuse atrophy. At 4 months of age, mild cardiac hypertrophy was seen on echocardiogram. The patient could not balance her head.

Lactic acidemia (4–9 mmol/L) with an elevated L/P ratio (20–25) and mild urinary excretion of methylmalonic acid persisted. An acylcarnitine profile of dried blood spots showed an increase in C3 (propionylcarnitine) and C4DC (isomers of methylmalonyl carnitine and succinylcarnitine). The serum level of methylmalonic acid was 13 μmol/L (control, not detected; MCM-deficient patients, 220–2900 μmol/L). The urinary levels of methylmalonic acid and methylcitrate were 321 mmol/molCr and 81.7 mmol/molCr, respectively (control, mean ± SD, 2.0 ± 1.2 mmol/molCr and 2.0 ± 0.9 mmol/molCr, respectively). A ^{14}C-propionate fixation assay using cultured fibroblasts showed that propionate fixation in the patient was 8% of that in the control. Enzymatic analyses of the pyruvate dehydrogenase complex and pyruvate carboxylase were normal.

Histology of a liver biopsy specimen indicated moderate macrovesicular and microvesicular steatosis in the hepatic parenchyma. There was no active inflammation or fibrosis. On electron microscopy hepatocytes containing lipid droplets were seen. Mitochondrial abnormalities and other specific findings were not apparent morphologically. Muscle biopsy samples were stained with hematoxylin and eosin, reduced nicotinamide adenine

dinucleotide tetrazolium reductase, modified Gomori-Trichrome, succinate dehydrogenase, periodic acid–Schiff, and cytochrome oxidase. No particular abnormalities were noted in the muscle biopsy specimens.

At 6 months of age, the patient was discharged from hospital. She was able to follow objects with her eyes. Because of feeding difficulty, a naso-gastric tube was used. She developed a social smile at 13 months of age but did not have head control. At 20 months of age, she suddenly died at home. Autopsy was not performed.

Because her clinical course was similar to that of previously reported SUCL-deficient patients,[3,4] we restarted diagnostic analysis using fibroblasts and biopsied muscle samples that had been stored for 16 years in liquid nitrogen.

Methods

Blue native polyacrylamide gel electrophoresis and Western blotting

Expression levels of the MRC complex (Co) I, II, III, and IV proteins in cultured fibroblasts were assessed on Western blotting using blue native polyacrylamide gel electrophoresis (BN-PAGE) according to previously described methods.[10] Immunostaining was performed using monoclonal antibodies specific for the 39 kD subunit of Co I, 70 kD subunit of Co II, core 1 subunit of Co III, and subunit 1 of Co IV (Invitrogen, Camarillo, CA, USA).

Determination of enzyme activities

Activities of MRC Co I, II, III, and IV were assayed.[10] The activity of each complex was presented as a percentage of the mean value obtained from 20 controls. The percentages of Co I, II, III, and IV activities relative to that of citrate synthase (CS) as a mitochondrial enzyme marker or Co II activity were calculated. Deficiency of each complex is confirmed when either the CS ratio and/or the Co II ratio is <45% (fibroblasts) or 35% (muscle).

Quantitative polymerase chain reaction

The mtDNA was quantitatively estimated on real-time amplification of ND1 fragments in the mtDNA genome, as described previously.[10] To determine the overall abundance of mtDNA, the real-time amplification result of ND1 was compared with that of exon 24 of the cystic fibrosis transmembrane conductance regulator (*CFTR*) gene, as nuclear DNA (nDNA).

Direct sequencing of the SUCLG1 and SUCLA2 genes

Genomic DNA was extracted from cultured fibroblasts using a Sepa Gene Kit (Sanko Junyaku, Tokyo, Japan). All coding exons, including flanking introns, in *SUCLG1* and the *SUCLA2* genes were amplified using polymerase chain reaction (PCR). To facilitate cycle sequencing analysis, M13 universal and reverse primer sequences were attached to the 5′ ends of sense primers and antisense primers, respectively. PCR products were directly sequenced using a Big Dye Primer Cycle Sequencing kit and an ABI 310 Genetic Analyzer (PE Applied Biosystems, Foster City, CA, USA).

The Ethics Committee of the Tohoku University School of Medicine approved the present study.

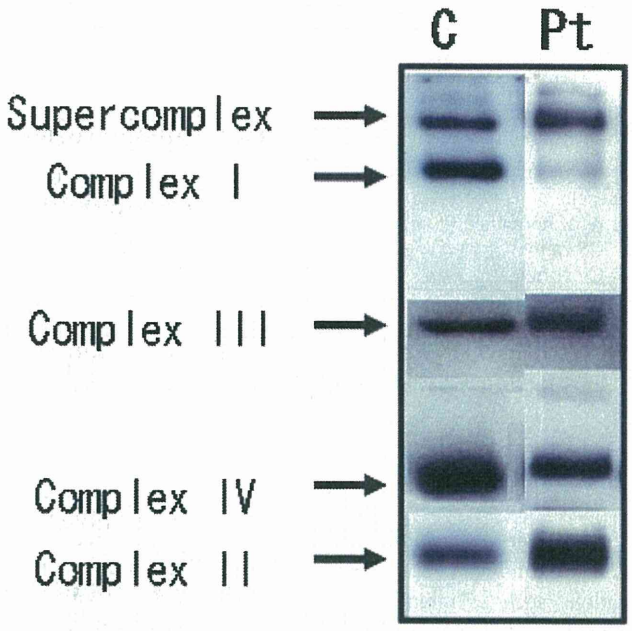

Fig. 1 Blue native polyacrylamide gel electrophoresis and subsequent Western blot analysis of mitochondrial respiratory chain complexes. The amount of assembled complex I was decreased. Complex I, anti-39 kDa subunit; complex II, anti-70 kDa subunit; complex III, anti-core 1 subunit; complex IV, anti-subunit 1.

Results

The amount of respiratory-chain complex in fibroblasts was determined on BN-PAGE Western blot. The intensity of the band corresponding to the assembled Co I of fibroblasts was decreased (Fig. 1). The intensity of the bands corresponding to Co II, III, and IV remained unchanged.

In fibroblasts, the enzyme activities of Co I and Co IV relative to that of Co II were decreased (<45%; Table 2). Even in the muscle biopsy samples, the ratios of (Co II + Co III)/CS, Co IV/CS, Co I/Co II, (Co II + Co III)/Co II, Co III/Co II, and CoIV/Co II were decreased.

Quantitative PCR showed that the ratio of mtDNA/nDNA of the fibroblasts did not decrease (72.9%; control, 76.4%). The ratio in the muscle biopsy specimen was also not decreased (270.1%).

Mutation analysis showed a heterozygous T-to-C substitution at position 41 in exon 1 of *SUCLG1* (c.41T > C; Fig. 2). This c.41T > C mutation changes the Met at position 14 to a Thr (p.M14T). Additionally, in exon 6, a heterozygous C-to-T substitution at position 599 in exon 1 of *SUCLG1* was found (c.599C > T). This mutation changes the Ser at position 200 to Phe (p.S200F). The p.M14T mutation was transmitted to the child from her mother; the other mutation (p.S200F) was transmitted to the child from her father (data not shown). Both substitutions were absent in the 100 alleles screened from healthy volunteers. No substitution was found in *SUCLA2*.

Table 2 Respiratory chain enzyme assay of the present patient

%	Co I	Co II	Co II + III	Co III	Co IV	CS
Fibroblasts						
% of normal	73	236	378	140	60	71
CS ratio	100	326	515	190	85	–
Co II ratio	**30**	–	158	58	**26**	–
Muscle						
% of normal	89	291	40	76	17	197
CS ratio	44	147	**20**	39	**8**	–
Co II ratio	**30**	–	**13**	**26**	**6**	–

Enzyme activities are expressed as % of mean normal control activity relative to protein, relative to CS, and relative to Co II. **Bold**, deficiency of the respective complex: <45% (fibroblasts) or 35% (muscle) of either CS ratio and/or Co II ratio. Reference range, fibroblasts 45–170; muscle 35–160.

Co I, complex I; Co II, complex II; Co III, complex III; Co IV, complex IV; CS, citrate synthase.

Discussion

The patient was identified to have a compound heterozygote mutation in *SUCLG1* (p.M14T and p.S200F). Clinical manifestations such as infantile lactic acidosis, mild methylmalonic aciduria, hypotonia, and hearing loss were compatible with symptoms previously reported in patients with *SUCLG1* or *SUCLA2* mutations.[3,6] The p.M14T and p.S200F mutations have not been reported previously. These substitutions were not found in the 100 alleles from healthy volunteers. p.M14 is located within the mitochondrial targeting sequence. Van Hove *et al.* reported a patient with a mutation at the same methionine (p.M14L) and speculated that the substitution of p.M14 would prevent proper translation initiation.[11] p.S200 is conserved across several species (Fig. 2). These data suggest that p.M14T and p.S200F are not polymorphisms but disease-causing mutations.

The amount of MRC complex I was decreased on BN-PAGE and Western blotting using fibroblasts, and multiple MRC defects were detected on enzyme assay. The ratios of mtDNA/nDNA of fibroblasts and muscle, however, did not decrease. Valayannopoulos *et al.* also reported that mtDNA depletion was not observed in two patients.[6] It is suggested that not all SUCL-deficient

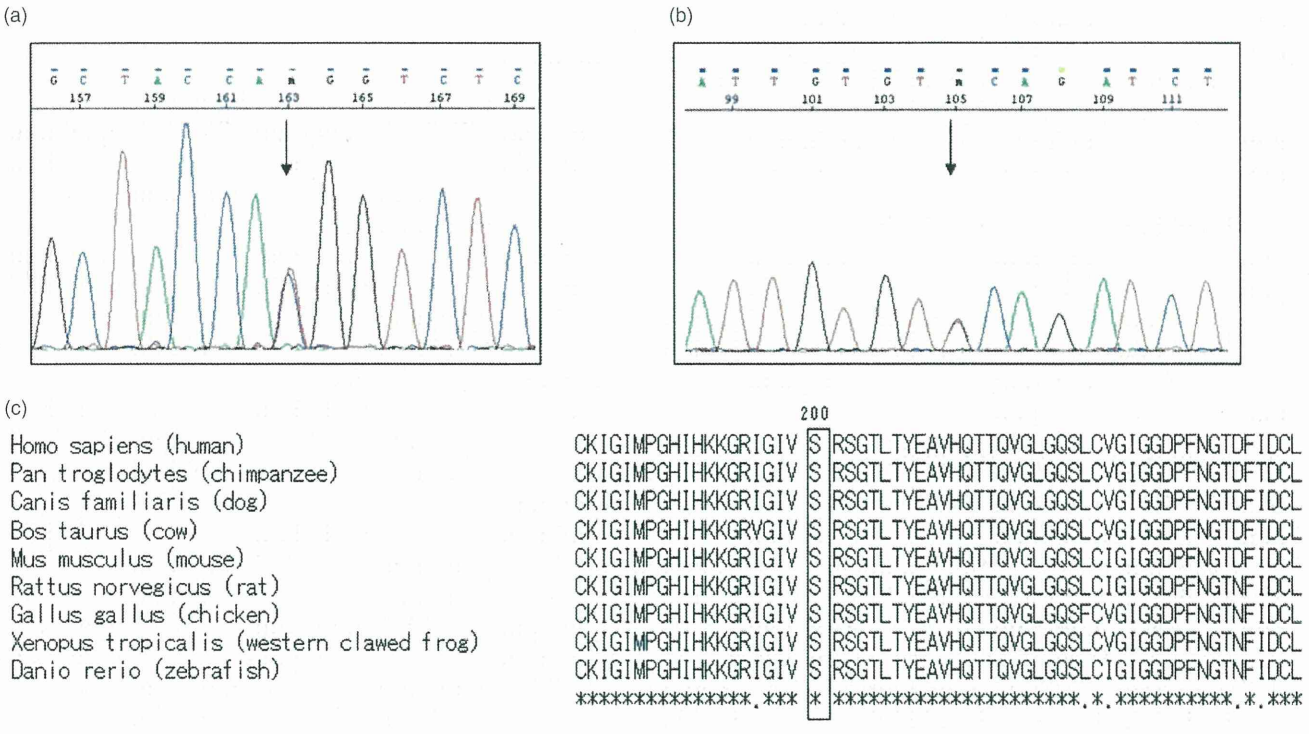

Fig. 2 (a) Heterozygous T-to-C substitution detected at c.41 in exon 1 of *SUCLG1*. This c.41T > C mutation changes the Met at position 14 to Thr (p.M14T). (b) Heterozygous C-to-T substitution detected at c.599 in exon 6 of *SUCLG1*. The c.599C > T substitution changes the Ser at position 200 to Phe (p.S200F). (c) Comparison of succinyl-coenzyme A ligase (SUCL) α subunits from several species. Serine at p.200 was conserved across all the species tested.

patients have mtDNA depletion, and that some mechanisms other than mtDNA depletion might participate in the multiple MRC deficiency observed in these patients.

In the present case, serum methylmalonic acid accumulation and low ^{14}C-propionate fixation capacity suggested disturbance of methylmalonic acid metabolism. Elevated methylmalonic acid may result from the accumulation of succinyl-coenzyme A under the assumption that accumulated succinyl-CoA inhibits the reaction catalyzed by MCM or causes an equilibrium shift, leading to the accumulation of methylmalonyl-coenzyme A, which is converted to methylmalonic acid. As usual, increased levels of C4DC are detected in patients with severe MCM deficiency during acute crises. It is suggested that the C4DC of the present patient was associated with an increased level of succinylcanritine due to accumulated succinyl-coenzyme A.

In conclusion, we identified two novel *SUCLG1* mutations in a Japanese female patient with neonatal lactic acidosis and prolonged mild methylmalonic aciduria. For patients showing these combined manifestations, MRC activities and mutations of *SUCLG1* or *SUCLA2* should be screened for.

Acknowledgments

We thank Dr Ichiki Kano (Sendai National Hospital) for providing clinical data, Drs Seiji Yamaguchi and Masahiko Kimura (Shimane University) for urinary organic acid analysis by gas chromatography and mass spectrometry, Dr Naoto Terada (Kyoto Prefectural University of Medicine) for acylcarnitine analysis by tandem mass spectrometry, and Drs Ichiro Yoshida and Syuichi Aramaki for quantitative analysis of methylmalonic acid. This work was partly supported by a grant from The Ministry of Health, Labor and Welfare of Japan.

References

1 Fenton WA, Gravel RA, Rosenblatt DS. Disorders of propionate and methylmalonate metabolism. In: Scriver CR, Beaudet AL, Sly WS, Valle D (eds). *The Metabolic and Molecular Bases of Inherited Disease*, 8th edn. McGraw-Hill, New York, 2001; 2165–93.
2 Ostergaard E. Disorders caused by deficiency of succinate-CoA ligase. *J. Inherit. Metab. Dis.* 2008; **31**: 226–9.
3 Elpeleg O, Miller C, Hershkovitz E *et al.* Deficiency of the ADP-forming succinyl-CoA synthase activity is associated with encephalomyopathy and mitochondrial DNA depletion. *Am. J. Hum. Genet.* 2005; **76**: 1081–6.
4 Ostergaard E, Christensen E, Kristensen E *et al.* Deficiency of the alpha subunit of succinate-Coenzyme A ligase causes fatal infantile lactic acidosis with mitochondrial DNA depletion. *Am. J. Hum. Genet.* 2007; **81**: 383–7.
5 Ostergaard E, Schwartz M, Batbayli M *et al.* A novel missense mutation in SUCLG1 associated with mitochondrial DNA depletion, encephalomyopathic form, with methylmalonic aciduria. *Eur. J. Pediatr.* 2010; **169**: 201–5.
6 Valayannopoulos V, Haudry C, Serre V *et al.* New SUCLG1 patients expanding the phenotypic spectrum of this rare cause of mild methylmalonic aciduria. *Mitochondrion* 2010; **10**: 335–41.
7 Rivera H, Merinero B, Martinez-Pardo M *et al.* Marked mitochondrial DNA depletion associated with a novel SUCLG1 gene mutation resulting in lethal neonatal acidosis, multi-organ failure, and interrupted aortic arch. *Mitochondrion* 2010; **10**: 362–8.
8 Randolph LM, Jackson HA, Wang J *et al.* Fatal infantile lactic acidosis and a novel homozygous mutation in the SUCLG1 gene: A mitochondrial DNA depletion disorder. *Mol. Genet. Metab.* 2011; **102**: 149–52.
9 Rouzier C, Le Guédard-Méreuze S, Fragaki K *et al.* The severity of phenotype linked to SUCLG1 mutations could be correlated with residual amount of SUCLG1 protein. *J. Med. Genet.* 2010; **47**: 670–76.
10 Kaji S, Murayama K, Nagata I *et al.* Fluctuating liver functions in siblings with MPV17 mutations and possible improvement associated with dietary and pharmaceutical treatments targeting respiratory chain complex II. *Mol. Genet. Metab.* 2009; **97**: 292–6.
11 Van Hove JL, Saenz MS, Thomas JA *et al.* Succinyl-CoA ligase deficiency: A mitochondrial hepatoencephalomyopathy. *Pediatr. Res.* 2010; **68**: 159–64.

ELSEVIER

Brain & Development 33 (2011) 753–757

BRAIN & DEVELOPMENT
Official Journal of the Japanese Society of Child Neurology

www.elsevier.com/locate/braindev

Review article

Two novel laboratory tests facilitating diagnosis of glycine encephalopathy (nonketotic hyperglycinemia)

Shigeo Kure *

Department of Pediatrics, Tohoku University School of Medicine, Sendai, Japan

Abstract

Glycine encephalopathy (GE), also known as non-ketotic hyperglycinemia, is a life-threatening metabolic disease caused by inherited deficiency of the glycine cleavage system (GCS). GE is characterized by accumulation of a large amount of glycine in serum and cerebrospinal fluids. In typical cases with GE, coma, profound hypotonia, and intractable seizures develop within several days of life. Patients with atypical symptoms may have delayed or missed diagnosis because of non-specific symptoms. It is sometimes problematic to confirm the diagnosis of GE since it requires either invasive liver biopsy for measurement of GCS activity or exhaustive mutational screening of three GCS genes, *GLDC*, *AMT*, and *GCSH*. We herein describe two novel laboratory tests for diagnosis of GE, [1-^{13}C]glycine breath test and the multiplex ligation-dependent probe amplification (MLPA) for detection of large deletions in *GLDC*. The [1-^{13}C]glycine breath test has been developed for noninvasive enzymatic diagnosis of GE. Because the GCS generates CO_2 by degradation of glycine, the GCS activity could be evaluated *in vivo* by measurement of exhaled $^{13}CO_2$ after administration of a stable isotope, [1-^{13}C]glycine. The MLPA has been developed for improvement in mutation detection rate in GE: Deletions involving multiple *GDLC* exons are prevalent among GE patients, but cannot be detected by the exon-sequencing analysis. Two novel diagnosis methods would facilitate diagnosis of hyperglycinemic patients as having GE.

Keywords: ^{13}C-glycine breath test; Decarboxylation of glycine *in vivo*; Detection of large deletions in *GLDC*; The MLPA analysis

1. Introduction

Glycine encephalopathy (GE, MIM 605899), also termed nonketotic hyperglycinemia (NKH), is an inborn error of glycine metabolism caused by deficiency of the glycine cleavage system (GCS) [1,2]. Typically, symptoms of GE start in the first days of life with progressive lethargy, hypotonia, myoclonoc jerks, hiccups, and apnea, usually leading to coma and death unless assisted ventilation and/or pharmacological treatment are provided [3]. Patients with atypical GE often lack neonatal symptoms, but present later with various neurological symptoms including seizures, motor and/or cognitive impairments, aggressive behavior, and impaired work or school performance [4–6]. Since these patients manifest only nonspecific clinical symptoms, their diagnosis may sometimes be delayed or missed and they may not benefit from early and appropriate management and counseling [7].

The GCS is a mitochondrial multi-enzyme complex that catalyzes the breakdown of glycine to carbon dioxide, ammonia, and one-carbon units (Fig. 1) [8]. The GCS is present in various animals, plants, and bacteria. In vertebrates, the activity of GCS has been reported in brain, liver, kidney, and testis [9]. The GCS consists of four individual proteins, glycine dehydrogenase (decarboxylating), aminomethyltransferase, glycine cleavage system H-protein and dihydrolipoamide dehydrogenase, which are encoded by distinct genes, *GLDC*,

* Address: Department of Pediatrics, Tohoku University School of Medicine, 1-1 Seiryomachi, Aobaku, Sendai 980-8574, Japan. Fax: +81 22 717 7290.
E-mail address: kure@med.tohoku.ac.jp

0387-7604/$ - see front matter © 2011 The Japanese Society of Child Neurology. Published by Elsevier B.V. All rights reserved.
doi:10.1016/j.braindev.2011.03.001

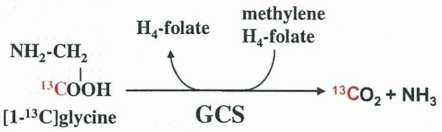

Fig. 1. Enzymatic reaction of the glycine cleavage system (GCS). One molecule of glycine is broken down, generating one molecule of carbon dioxide, ammonia, and one carbon unit. Note that $^{13}CO_2$ is synthesized from [1-^{13}C]glycine.

AMT, *GCSH* and *DLD*. Dihydrolipoamide dehydrogenase is a so-called housekeeping enzyme that serves as a component of other complex enzyme systems such as the pyruvate dehydrogenase complex and the branched chain ketoacid dehydrogenase complex. No participation of other GCS components to other enzyme system has been reported to date.

Diagnosis of GE should be considered when neonates or infants develop seizures, muscular hypotonia, and lethargy that are not readily explicable on the basis of infection, trauma, hypoxia, or other commonly encountered pediatric problems. Differential diagnosis between GE and other diseases with hyperglycinemia is sometimes difficult. The absence of ketoacidosis is indicated by plasma biocarbonate levels and/or blood pH. Exclusion of organic acidemia by gas chromatographic analysis of urine or plasma are crucial [10]. In GE the glycine level in cerebrospinal fluids (CSF) is elevated and the ratio of CSF to plasma glycine concentration is increased more than 0.09, while in normal and ketotic hyperglycinemia it is below 0.04. An EEG finding of a burst suppression pattern is characteristic to GE in the first month of life.

As the clinical picture of GE is so highly heterogeneous, it may sometimes be difficult to diagnose GE solely on the basis of clinical symptoms and the amino acid analysis of CSF and serum. Atypical GE patients can have some residual GCS activities, as demonstrated by enzymatic analysis of GCS activity in liver samples [11] and by *in vitro* expression analysis of the identified mutations [6,12]. The elevations of glycine concentrations and the CSF/plasma glycine ratio in atypical GE are milder than those in typical cases. Furthermore, increased glycine levels and ratio have also been observed in other pathological conditions or as a result of technical artifacts or administration of certain drugs [10]. Therefore, the clinical diagnosis requires confirmation either by enzymatic analysis of the GCS in liver tissues obtained by invasive biopsy or the exhaustive mutational analysis of three responsible genes, *GLDC*, *AMT*, and *GCSH*. Both procedures are laborious, and require technical expertise, and are currently performed in only a limited number of laboratories.

Here we report a recent advance in diagnosis of GE by introdicing two novel diagnostic methods, the ^{13}C-glycine breath test and the multiplex ligation dependent probe amplification (MLPA) method for detection for large deletions in *GLDC*. Both methods would facilitate confirmation of diagnosis of GE in patients with hyperglycinemia.

2. ^{13}C-glycine breath test facilitating enzymatic diagnosis of GE

2.1. Principle of the ^{13}C-glycine breath test

The activity of the GCS is currently measured *in vitro* by measuring the radioactivity of $^{14}CO_2$ generated from substrate, [1-^{14}C]glycine [11]. When glycine is administered to normal subjects, it is decarboxylated predominantly by the GCS in liver, leading to production of CO_2. The amount of CO_2 production may be easily quantified if glycine is labeled with stable isotope, [1-^{13}C]glycine. ^{13}C is not radioactive, and can be safely administered to patients including children [13]. Since the generated $^{13}CO_2$ is excreted into exhaled breath one can evaluate the GCS activity *in vivo* by gathering exhaled breath for measurement of concentration of $^{13}CO_2$ [14].

2.2. Method of [1-^{13}C]glycine breath test

The procedure of [1-^{13}C]glycine breath test is shown in Fig. 2. [1-^{13}C]glycine with >99% purity is used for the breath test. The ^{13}C-glycine is administered orally at a dose of 10 mg/kg, a maximum dose of 100 mg. In the case that a subject is an infant or small child or a mentally-retarded child it is administered through gastric tubes. Before the administration of ^{13}C-glycine, a reference breath sample was collected by using a facemask equipped with a one-way air valve followed by transfer to the sampling bags. Test samples of 150–250 ml were collected from each subject at 15, 30, 45, 60, 90, 120, 180, 240, and 300 min after the administration of ^{13}C-glycine. The difference of $^{13}CO_2$ concentration ($\Delta^{13}CO_2$) between reference and test breath samples was measured using an infrared $^{13}CO_2$ analyzer, UBit-IR300 (Otsuka Electronics, Osaka, Japan) [15]. Cumulative %recovery was calculated from administered dose (mg) of ^{13}C-glycine, $\Delta^{13}CO_2$ values (‰), body weight (kg), and body length (cm) as described [14].

2.3. Reliability of the ^{13}C-glcyine breath test

The breath test was performed in a total of 10 control subjects: 24.1 ± 4.0% of ^{13}C was recovered within 5 h after administration of ^{13}C-glycine. The ^{13}C-glycine breath test was previously performed in neonates for evaluation of gastric emptying time [16]. The cumulative ^{13}C recovery at 300 min after ^{13}C-glycine administration was 21.5 ± 4.3% in healthy neonates, similar to that in our study. We therefore used 24.1 ± 4.0% as the

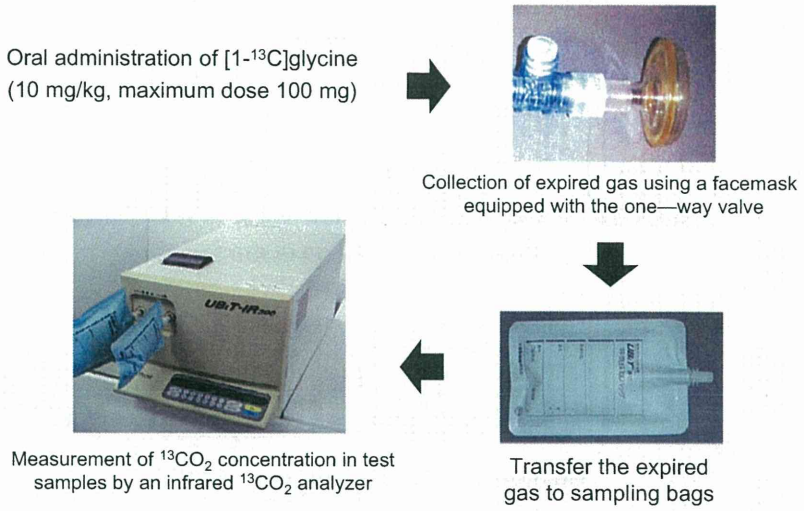

Fig. 2. Procedure of the ^{13}C-glycine breath test. After the oral administration of [1-^{13}C]glycine, expired gas of a subjects is collected with the facemask at each time point, which are subjected to measurement of $^{13}CO_2$ level by the infrared $^{13}CO_2$ analyzer.

control value. The breath test was then performed in five patients with GE. Their mean cumulative recovery was 8.3 ± 2.3%, which was significantly lower than that in control subjects ($p < 0.0001$). Therefore, patients with GE could be readily distinguished from non-GE individuals. In contrast, the mean cumulative recovery in seven obligate carriers, the parents of the patients, was 22.9 ± 3.3%, which is not significantly different from the control subjects, suggesting that carrier detection is extremely difficult. Patients with organic acidemia such as methylmalonic acidemia (MMA) or propionic academia are known to show secondary hyperglycinemia. A patient with MMA showed 18.1% cumulative recovery, which was slightly lower than the control mean by 1.3 SD. The GCS activity in liver specimens was reported in three patients with organic acidemia [17]. One patient on a low-protein diet had normal GCS activity in his biopsied liver sample. Two other patients who died with severe metabolic acidosis had markedly low GCS activities in their autopsied liver, suggesting that the hepatic GCS activity in patients with organic acidemia may be influenced by their metabolic status. Since the ^{13}G-glycine breath test reflects the in vivo GCS activity, its result in patients with organic acidemia may fluctuate depending on their condition at the time of the test.

2.4. Utility of the ^{13}C-glycine breath test

The ^{13}C-glycine breath test is an in vivo assay of the GCS activity, which enables the rapid and reliable diagnosis of GE. The ^{13}C-glycine breath test can be easily performed in neonates, small children and adult patients. The ^{13}C-glycine stable isotope is not toxic. It has the advantages of being simple, non-invasive and widely available. Recently, a simple and inexpensive $^{13}CO_2$ analyzer using infrared spectrophotometry has been developed for the diagnosis of *Helicobacter pylori* infection by the ^{13}C-urea test [18]. Since the infrared $^{13}CO_2$ analyzer is now widely distributed, the ^{13}C-glycine breath could be readily accomplished in many hospitals and clinics. Diagnosis of atypical GE cases is often difficult by amino acid analysis alone as the CSF/plasma glycine ratio is not as high in atypical cases [4]. Since the assay conditions for measuring GCS activity differ in detail from laboratory to laboratory, it is difficult to compare the results from different laboratories. In contrast, the protocol for the ^{13}C-breath test is readily standardized. It could become a standard test for the evaluation of the GCS activity, and facilitate early diagnosis of atypical GE.

3. MLPA analysis facilitating genetic diagnosis of GE

3.1. Mutations in the GCS genes

The GCS has three specific components encoded by GLDC, AMT, and *GCSH*. A comprehensive screening was performed for *GLDC*, *AMT*, and *GCSH* mutations in 56 patients with neonatal GE [19]. The *GLDC* mutations were identified in 36 of 56 (64%) patients while the AMT mutations were found in 6 of 56 patients (11%). No mutation was identified in *GCSH*. Both *GLDC* and *AMT* mutations were highly heterogeneous, including many private mutations. To our best knowledge, there are only two prevalent mutations, p.S564I in Fins [20] and p.R515S in Caucasians [21]. In 16 of the 36 (44%) patients with the *GLDC* mutations, mutations could be identified in only one allele despite extensive sequencing of the entire coding regions, suggesting that there are *GLDC* mutations that cannot be detected by the exon-sequencing method.

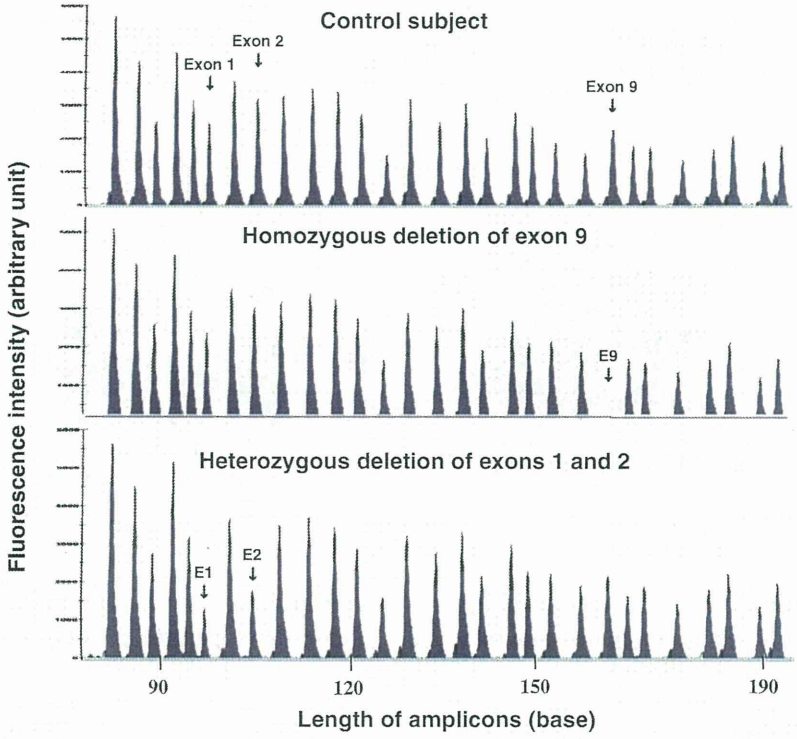

Fig. 3. Chromatogram of the multiplex ligation-dependent probe amplification (MLPA) analysis of a control subject and two GE patients. The horizontal axis indicates length of the PCR product and the vertical axis represents fluorescence intensity of each DNA fragment. A DNA fragment corresponding to GLDC exon 9 in a control subject (panel A) is completely missing in a GE patient with homozygous deletion of *GLDC* exon 9 (panel B). The peak areas of exons 1 and 2 are reduced in a GE patient with heterozygous deletion of *GLDC* exons 1 and 2 (panel B), compared with those in a control subject (panel A).

3.2. Detection of large deletion in GLDC by MLPA method

We previously encountered several patients with deletion of *GLDC* exon 1 [22]. Sellner et al. have reported a patient with deletion of the *GLDC* exons 2–15 [23]. Those observations suggested that a considerable number of *GLDC* deletions may remain unidentified. We have developed a screening system for deletions in *GLDC* by the MLPA method [24]. The MLPA method uses a pair of oligonucleotide probes, upstream and downstream probes, for each GLDC exon. The upstream probe is designed to locate in adjacent to the downstream probes. After hybridization of the oligonucleotide probes with the genomic DNA the hybridization mixtures are subject to ligation reaction. The upstream and downstream probes can be ligated only when they are hybridized with their target sequences. Both upstream and downstream probes have binding sequence for the universal PCR primers, which enables us to amplify the ligated probes by PCR with the universal primers. Allele number of each target exon can be evaluated by measuring amount of PCR products amplified from each ligated probes.

3.3. Screening of GLDC deletions in GE patients

Two distinct cohorts of patients with typical GE were screened by this MLPA method [24]: the first cohort consisted of 45 families with no identified *AMT* or *GCSH* mutations. The second cohort was comprised of 20 patients from the UK who were not prescreened for *AMT* mutations. Deletions in *GLDC* were identified in 16 of 90 alleles (18%) in the first cohort and 9 of 40 alleles (22.5%) in the second cohort. A total of 14 deletions with various lengths were identified, varying from a single exon to entire GLDC gene. Typical result of the MLPA analysis in the GE patients is shown in Fig. 3. Sequencing analysis of the flanking sequences of several deletions suggested that *Alu*-mediated recombination may underlie in the etiology of the *GLDC* deletions.

3.4. Utility of the MLPA test

Mutations in the GCS genes are highly heterogeneous in GE, suggesting necessity of sequencing entire coding regions of the GCS genes for genetic confirmation of GE. Full sequencing of three GCS genes is, however, too lengthy to perform for the clinical genetic testing